Science of the Total Environment 902 (2023) 166003

Contents lists available at ScienceDirect

Science of the Total Environment

journal homepage: www.elsevier.com/locate/scitotenv

Simulated gastrointestinal digestion of polylactic acid (PLA) biodegradable microplastics and their interaction with the gut microbiota

C. Jiménez-Arroyo [a], A. Tamargo [a], N. Molinero [a], J.J. Reinosa [b,c], V. Alcolea-Rodriguez [d], R. Portela [d], M.A. Bañares [d], J.F. Fernández [c], M.V. Moreno-Arribas [a,*]

[a] Institute of Food Science Research, CIAL, CSIC-UAM, C/ Nicolás Cabrera 9, 28049 Madrid, Spain
[b] Instituto de Cerámica y Vidrio, CSIC, c/ Kelsen, 28049 Madrid, Spain
[c] Encapsulae S.L., c/Lituania 10, 12006 Castellón de la Plana, Spain
[d] Instituto de Catálisis y Petroleoquímica, CSIC, c/ Marie Curie, 2, 28049 Madrid, Spain

HIGHLIGHTS

- Ingested PLA particles showed several biotransformations in the gastrointestinal tract.
- PLA exposure leads to structural and functional alterations in human gut microbiota.
- Microbial biofilms on PLA MPs surface suggest colonic microbiota colonization.
- Bifidobacteria and pullulanase activity seems to be associated to PLA ingestion.
- Exposure to bioplastics and their potential health effects merits critical investigation.

GRAPHICAL ABSTRACT

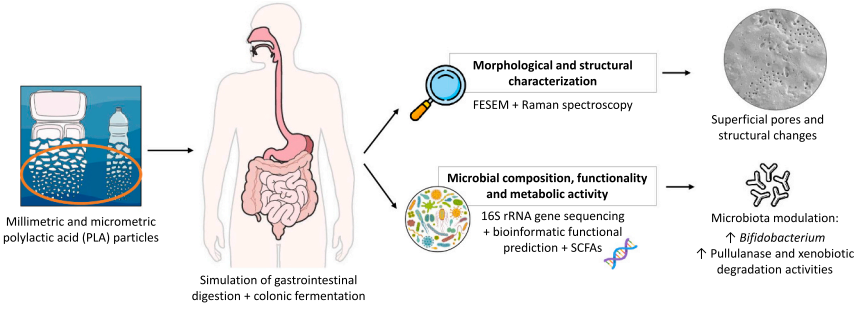

ARTICLE INFO

Editor: Damia Barcelo

Keywords:
Bioplastics
Microplastics
PLA
Human digestion
Gut microbiome
Health
Raman
SEM
Biodegradation

ABSTRACT

The accumulation of microplastics (MPs) in the environment as well as their presence in foods and humans highlight the urgent need for studies on the effects of these particles on humans. Polylactic acid (PLA) is the most widely used bioplastic in the food industry and medical field. Despite its biodegradability, biocompatibility, and "Generally Recognized As Safe" (GRAS) status, recent animal model studies have shown that PLA MPs can alter the intestinal microbiota; however, to date, no studies have been reported on the possible gut and health consequences of its intake by humans. This work simulates the ingestion of a realistic daily amount of PLA MPs and their pass through the gastrointestinal tract by combining the INFOGEST method and the gastrointestinal simgi® model to evaluate possible effects on the human colonic microbiota composition (16S rRNA gene sequencing analysis) and metabolic functionality (lactic acid and short-chain fatty acids (SCFA) production). Although PLA MPs did not clearly alter the microbial community homeostasis, increased *Bifidobacterium* levels tended to increase in presence of millimetric PLA particles. Furthermore, shifts detected at the functional level suggest an alteration of microbial metabolism, and a possible biotransformation of PLA by the human microbial colonic

Abbreviations: MPs, microplastics; PS, polystyrene; PE, polyethylene; PVC, polyvinyl chloride; PET, polyethylene terephthalate; PLA, polylactic acid; FESEM, field emission scanning electron microscopy; SSF, simulated salivary fluid; SGF, simulated gastric fluid; SIF, simulated intestinal fluid; TSA, trypticase soy agar; TSC, tryptose sulphite cycloserine; SCFAs, short-chain fatty acids; ASVs, amplicon sequence variants.

* Corresponding author.
E-mail address: victoria.moreno@csic.es (M.V. Moreno-Arribas).

https://doi.org/10.1016/j.scitotenv.2023.166003
Received 25 May 2023; Received in revised form 6 July 2023; Accepted 25 July 2023
Available online 6 August 2023

community. Raman spectroscopy and field emission scanning electron microscopy (FESEM) characterization revealed morphological changes on the PLA MPs after the gastric phase of the digestion, and the adhesion of organic matter as well as a microbial biofilm, with surface biodegradation, after the intestinal and colonic phases. With this evidence and the emerging use of bioplastics, understanding their impact on humans and potential biodegradation through gastrointestinal digestion and the human microbiota merits critical investigation.

1. Introduction

The extensive use of plastic products over recent decades, with the lack of multinational/global approaches for recycling and upcycling, has led to the irreversible accumulation of plastics of various sizes and blends in most environments and ecological niches (Allen et al., 2022; Gewert et al., 2015). Microplastics (MPs), plastic particles smaller than 5 mm that can be intentionally manufactured on that scale (primary MPs) or derived from larger plastics (secondary MPs), contaminate all known ecosystems, reaching the human body mainly by ingestion, although other possible routes have been proposed (Kutralam-Muniasamy et al., 2023; Malafaia and Barceló, 2023; Ramsperger et al., 2023; Senathirajah et al., 2021).

The detection of MPs in commonly consumed food and beverages, and in the food system (Rubio-Armendáriz et al., 2022; Toussaint et al., 2019; Wen et al., 2022), as well as in human feces (Schwabl et al., 2019; Yan et al., 2022a; Zhang et al., 2021b; Zhang et al., 2021c) supports the hypothesis of their interaction with the digestive system. However, to date, only a handful of publications have addressed the consequences of MP ingestion and gastrointestinal digestion for humans or their potential effects on the gut microbiome and overall health. The studies conducted so far in mice and other animal models have reported that ingested MPs could decrease the richness and diversity of intestinal bacterial communities, as well as alter their taxonomic composition and metabolic function (Jin et al., 2019; Lu et al., 2018; Ouyang et al., 2021; Zhang et al., 2021d; Zhao et al., 2021). However, these works rarely evaluate the digestion process and have been almost exclusively focused on durable, petroleum-based, and non-biodegradable polymers such as polystyrene (PS; Qiao et al., 2021), polyethylene (PE; Chen et al., 2022a), and polyvinyl chloride (PVC; Chen et al., 2022b). In vitro models that mimic the physiological conditions occurring during human digestion are useful tools to investigate changes, interactions, and bioaccessibility of nutrients, drugs, and non-nutritive compounds, including nanomaterials and plastics of different sizes (Cueva et al., 2019; Fournier et al., 2021; Jiménez-Arroyo et al., 2023). However, the understanding of MPs-gut interactions in physiological model systems is also limited to a few types of MP polymers—mainly polyethylene terephthalate (PET) and PS—and some gut conditions, mainly static digestion and, to a lesser extent, the inclusion of colonic fermentation (Godoy et al., 2020; Huang et al., 2021a; Tamargo et al., 2022; Tan et al., 2020).

In recent decades, the environmental and public health impact of plastics and MPs has become an undeniable critical challenge, which has led to the development of biodegradable polymers. Polylactic acid (PLA, $[–C(CH_3)HC(=O)O–]_n$), with an annual production of ca. 0.4 million tons per year, is the most commonly used bio-based polymer or "bioplastic," which can be found in food packaging, 3D-printed gadgets, disposable plastic tableware materials and textile fibers, as well as in biomedical devices and surgical procedures because of its biodegradable and bioresorbable nature (DeStefano et al., 2020; Farah et al., 2016; Pang et al., 2010). PLA biocompatibility has been known for decades and has been tested both in vitro and in vivo (Athanasiou et al., 1996; Elmowafy et al., 2019). Furthermore, to the best of our knowledge, no accumulation in the human body has ever been described by this polymer when used in low concentrations. However, some behavioral changes and biochemical dysfunctions caused by PLA MPs have recently been demonstrated in different aquatic animals, such as tadpoles (Malafaia et al., 2021), adult zebrafish (Chagas et al., 2021b), larval zebrafish (de Oliveira et al., 2021), and larval dragonflies (Chagas et al., 2021a). Furthermore, exposure to PLA MPs also significantly affects intestinal microbial communities of animal intestines, e.g., zebrafish, *Danio rerio* (Duan et al., 2022) and earthworms, *Eisenia fetida* (Yu et al., 2022). Therefore, despite its GRAS (Generally Recognized As Safe) status, the potential effects of PLA MPs' ingestion and digestion at the gut level must be assessed.

We hypothesized that ingestion of PLA MPs and their accumulation in the digestive tract could affect gastrointestinal digestion processes and the gut microbiome in vitro under realistic conditions. Therefore, the aim of this work is to study the impact of gastrointestinal digestion and colonic fermentation on PLA MPs from a bidirectional viewpoint. Thus, we provide scientific evidence about the modifications and effects of millimetric and micrometric PLA ingested in a realistic amount during their passage through the human digestive tract. Upper digestion was simulated in a standardized in vitro static model and colonic-microbial fermentation in the Dynamic SIMulator of the GastroIntestinal tract (simgi®) [https://www.cial.uam-csic.es/simgi/index_eng.html]. Furthermore, changes in gut microbiota composition (microbial counts and 16S rRNA gene-based metagenomic analysis), microbial activity (lactate and short-chain fatty acid production), and PLA particles morphology, as well as microbial aggregation/colonization on them, were evaluated in the different digestion phases (oral, gastric, intestinal, and colonic).

2. Materials and methods

2.1. Polylactic acid (PLA) microplastics origin

The net PLA commodity was used without additional processing additives that could distort its crystallinity or chemical reactivity. Two microparticle sizes were selected for the study: as received commercial granular PLA millimetric pellets or PLAg (PLA, ErcrosBio® LL 650, Ercros, Spain, d ca. 5 mm) and milled micrometric PLA or PLAm ($d = 240 \pm 65$ μm) obtained by blade milling of PLAg in liquid nitrogen (FRITSCH Pulverisette 11, Germany).

2.2. PLA characterization

Original PLAg pellets and derived PLAm MPs, as well as samples of both types of PLA collected during the stages of gastrointestinal digestion (oral, gastric, and small intestine phases) and after 72 h colonic fermentation were characterized using microscopic and spectroscopic techniques. The samples were gold coated (≈200 Å) for size and morphology examination by field emission scanning electron microscopy (FESEM) (Hitachi S-4700, Japan) at 5 keV and optical analysis in a Multimode Optical Profilometer (Zeta-20, Zeta Instruments, USA). Before coating, to better observe possible biofilms formed on the PLAg and PLAm surface and preserve the microbial structure, colon samples were washed twice with sterile PBS 1× and fixed for 3 h in a solution of 2 % glutaraldehyde (Sigma-Aldrich, USA) and 1 % paraformaldehyde (Sigma-Aldrich) in sterile PBS 2×. The samples were conserved in absolute ethanol at 4 °C until analysis.

The structural changes of PLA caused by the cryomilling procedure as well as by gastrointestinal digestion and colonic fermentation were evaluated by micro-Raman mapping using a Renishaw InVia Qontor spectrometer. Each spectrum comprised 120 accumulations of 1 s with a laser power of 1.5 mW. First, the surface of each sample was mapped on at least 60 points with a 514 nm excitation line laser using a 50× microscope objective to generate data representative of the state of the sample. Then,

at selected points of each sample, where PLA surfaces showed spectral changes, a depth profile was measured at 1 μm steps from the surface to the bulk with a 405 nm excitation line laser using a 100× microscope objective in confocal configuration. Every sample was mapped on at least 20 points per depth layer to generate a representative depth profile.

2.3. In vitro static gastrointestinal digestions

The selected PLAg and PLAm MPs dose for gastrointestinal digestion was based on the estimated mean dietary consumption value for humans, 0.166 g/intake, as in our previous study on PET MPs (Tamargo et al., 2022) (Fig. 1). Gastrointestinal digestions were performed using the INFOGEST method (Brodkorb et al., 2019) in triplicate. Briefly, the MPs were suspended in Milli-Q water until 2 g of food dose was reached. To simulate the oral phase, they were mixed at 1:1 with simulated salivary fluid (SSF) and incubated on an orbital shaker for 2 min at 37 °C. Then, simulated gastric fluid (SGF) and commercial porcine pepsin were added, providing an enzymatic activity of 2000 U/mL in the final digestion mixture. The pH was adjusted to 3, and the samples were incubated for 120 min at 37 °C with continuous agitation. After the gastric stage, simulated intestinal fluid (SIF) was added and the digested samples were set to pH 7. Finally, the intestinal phase was simulated by adding bile salts and pancreatin to reach 100 U/mL of trypsin activity and 10 mM of bile salts in the final mixture, which was incubated in the same conditions for 120 more minutes. To stop the digestion process, the samples were immediately frozen for 24 h and kept at −20 °C until posterior use in colonic fermentations.

2.4. In vitro colonic fermentation using simgi®

Colonic fermentations using human colonic microbiota were conducted in the simgi® system in triplicate. Simgi® is a computer-controlled dynamic simulator of the gastrointestinal tract comprising five successive reactors that can reproduce gastrointestinal digestion and colon fermentation (Cueva et al., 2015). In this study, the three colonic reactors were used as three independent batch reactors kept at 37 °C and 150 rpm in anaerobic conditions for colonic fermentation simulation. The pH was maintained at 6.3 by automatically adding 0.5 M NaOH and HCl in each reactor. Flow rates, compartment volumes, pH, and temperature were computer-controlled during the experiments. Each reactor was filled with 300 mL of Gut Nutrient Medium (GNM) containing arabinogalactan (1 g/L), citrus peel pectin (2 g/L), xylan (1 g/L), potato starch (3 g/L), glucose (0.4 g/L), yeast extract (3 g/L), peptone (1 g/L), mucin (4 g/L), and L-cysteine (0.5 g/L). Each of the three colonic compartments was inoculated with a 20 % (*w/v*) fresh fecal suspension from a different healthy volunteer (fecal inoculum) prepared as described by Tamargo et al. (2018) to study the colonic fermentation of volunteers 1, 2 and 3. Immediately, the reactors were fed with a single dose (0.166 g) of one of the different digested samples: digested PLAm, digested PLAg, or the blank of gastrointestinal digestion (as a colonic fermentation control). The colonic fermentation conditions were kept for 72 h. Samples from the three simgi® reactors were collected before feeding (0 h) and after colonic fermentation for 24, 48, and 72 h. The experimental protocol with fecal human samples was approved by the Ethics Committee of the Spanish National Research Council (CSIC)

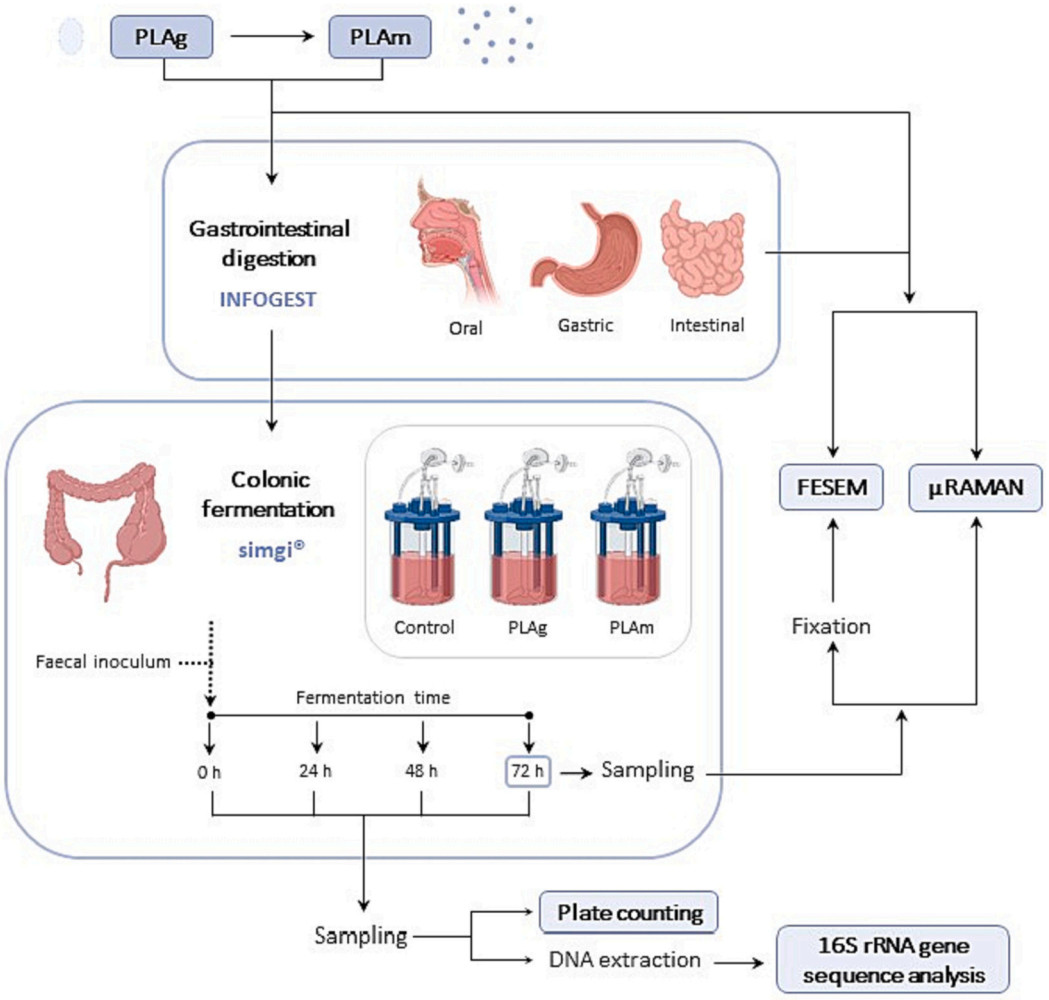

Fig. 1. Experimental set-up of the study.

(registration code AGL2015–64522), and was consistent with the Declaration of Helsinki. The signed informed consent of the donors was obtained at the time of enrolment.

2.5. Colonic microbiota analysis

2.5.1. Plate counting

Immediately after each sampling step, tenfold serial dilutions of PLAg, PLAm, and control simgi® samples were plated on different types of selective media as described before (Tamargo et al., 2018). Briefly, Trypticase Soy Agar (TSA) (Difco™, BD, USA) was used as media for total aerobes plate counting, Wilkins Chalgren agar (Difco™, BD) for total anaerobes, MacConkey agar (Difco™, BD, USA) for *Enterobacteriaceae*; Enterococcus agar (Difco™, BD, USA) for *Enterococcus* spp., MRS agar (pH = 5.4) (Pronadisa, CONDA, Spain) for lactic acid bacteria, Tryptose Sulfite Cycloserine agar (TSC) (Pronadisa, CONDA, Spain) for *Clostridium* spp., BBL CHROMAgar Staph aureus (Difco™, BD, USA) for *Staphylococcus* spp., Bifidobacterium agar modified by Beerens (Difco™, BD, USA) for *Bifidobacterium* spp., and LAMVAB for specific fecal *Lactobacillus* spp. All plates were incubated at 37 °C for 24 to 72 h under anaerobic conditions (BACTRON Anaerobic Environmental Chamber, SHELLAB, USA), except for BBL CHROMAgar Staph aureus and TSA, which were incubated under aerobic conditions. Plate counting was performed in triplicate and the data was expressed as log (CFU/mL).

2.5.2. DNA extractions from colonic samples and Illumina MiSeq sequencing

Two milliliter samples from PLAm, PLAg, and control simgi® reactors at different sampling times were used for DNA extraction using the QIAamp DNA Stool Mini Kit (Qiagen, Hilden, Germany). The V3-V4 region of the 16S ribosomal RNA gene was amplified using forward 5'-CCTACGGGNBGCASCAG-3′ and reverse 5'-GACTACNVGGGTATCTAATCC-3′ primers. The two-step Illumina® PCR protocol was followed to prepare the libraries, and the samples were submitted to 2 × 500 bp paired-end sequencing with an Illumina® MiSeq instrument (Illumina®, USA). The RStudio v.1.3.1093 software was used to process the files with raw reads from the Illumina® instrument. The fastqc files were filtered for reads of low quality and the presence of alien DNA using DADA2. The DADA2 algorithm was also employed to denoise, join paired-end reads, and filter out chimeras in the raw data (Callahan et al., 2016a; Callahan et al., 2016b). This algorithm allows the differentiation of even a single nucleotide, helping to form Amplicon Sequence Variants (ASVs). Taxonomic assignment was performed using the naïve Bayesian classifier implemented in DADA2 using Silva v.138 as a reference database (Quast et al., 2013), with a bootstrap cut-off of 80 %. A total of 1511 ASVs were found. Biodiversity, expressed in terms of alpha-diversity, was estimated using ASVs by calculating the Observed, Shannon, and Simpson indices through the "Phyloseq" package. Beta diversity was evaluated using a Bray-Curtis dissimilarity matrix represented by non-metric multidimensional scaling (NMDS).

2.6. Colonic metabolism analysis

Two milliliter samples of PLAm, PLAg, and control simgi® reactors were used at different sampling times to determine lactate and short-chain fatty acids (SCFA). The samples were centrifuged at 10,000 rpm and 4 °C for 10 min and the resulting supernatants were filtered by 0.22 μm. Lactate was analyzed by ionic chromatography and SCFAs by GC–MS (Cueva et al., 2015; García-Villalba et al., 2012).

2.7. Statistical analysis

A two-way ANOVA test and the Games-Howell post hoc test were used for all statistical analyses to study differences between samples (PLAm, PLAg, and the control) and their changes at colonic fermentation time. Significant differences were determined considering p-adjust <0.05 with the XLSTAT Statistic software for Microsoft Excel, 2022.3.1 (Addinsoft-SARL, USA). A functional prediction was conducted with the *Tax4Fun2* package in R statistical software version 4.2.2 and RStudio 2022.07.2 (https://www.r-project.org/), using the Ref99NR dataset. For the statistical analysis of functional prediction, the non-parametric Wilcoxon test with Bonferroni correction was applied. The results were considered statistically different from the control when $q < 0.05$.

3. Results

3.1. Effect of gastrointestinal digestion and colonic fermentation on PLA morphology

Changes in the PLA surface after each gastrointestinal digestion step were examined by FESEM (Fig. 2). Raw PLAg polymer, as rounded pellets with dimensions of a few millimeters (ca. 3.4 mm), shows a relatively smooth surface (Fig. 2A), with defects generated by the cutting process and attrition during the pellets processing and transportation. An examination at higher magnifications reveals the presence of regions with small spherulites characteristic of PLA crystallization (Fig. 2A insert). The cryomilling process to generate PLAm produces irregular surfaces (Fig. 2B) with folds and tears characteristic of a material fracture with plastic deformation. PLA has a mechanical resistance similar to that of polymeric materials, such as PET. However, its elongation at break is much lower; therefore, it is a rigid polymer with brittle breakage fracture (Sangeetha et al., 2018). The PLA glass transition temperature is ca. 58 °C, and therefore cryomilling does not prevent plastic deformation during the microparticle generation processes because local heating cannot be avoided. After the oral phase, crystalline deposits are apparent on the PLA surfaces, but no other significant changes were observed (Fig. 2C, D). During the roughness of the gastric phase, the surface was altered, and pits and pores were formed on the surface of both PLAg and PLAm, probably because of the hydrolysis of some ester bonds in the acid media of the digestion process (Fig. 2E, F). However, the size and concentration of the perforations appear dependent on the particle texture: thus, they were few but large for PLAg, whereas they were small but numerous for PLAm. Both the appearance of pores and the modification of the surface roughness are consistent with an increasing degradation of polymeric materials. After the intestinal phase, salt and organic matter deposits are apparent on the particle surfaces of both series (Fig. 2G, H). Finally, the colonic fermentation stage renders high morphological particle irregularity, uncovering a more extended surface degradation of PLA particles. Furthermore, organic matter deposits and a microbial biofilm were observed on the polymer surface. The formation of this biofilm suggests colonization of the particles by the colonic microbiota (Fig. 2I-L).

3.2. Effect of gastrointestinal digestion and colonic fermentation on PLA structure

The degradation and crystalline state of PLA was monitored by Raman spectroscopy (Fig. 3). The assignment of PLA Raman bands can be found elsewhere (Yuniarto et al., 2016). The strong Raman mode at 873 cm^{-1}, corresponding to backbone vs. C-COO in PLA, has been used to normalize Raman spectra (Kister et al., 1998, 2000). Sixty representative spectra of PLAg show no appreciable differences (Fig. 3A), in line with the homogeneity observed in FESEM. In the case of PLAm before GI stages, the slight variability between the 60 Raman spectra (Fig. 3B) indicates structural changes in PLA due to the cryomilling process, in line with the incipient modification illustrated by FESEM. The Raman spectra of PLAg and PLAm samples after the oral phase (Fig. 3C and D, respectively) hardly show any difference in their fresh counterparts, in line with FESEM micrographs that only show the accumulation of some salts at the surface of the particle, whereas the materials remain essentially unchanged. The Raman spectra of PLAg after gastric and intestinal digestion and colonic fermentation stages (Fig. 3E, G, I) indicate again

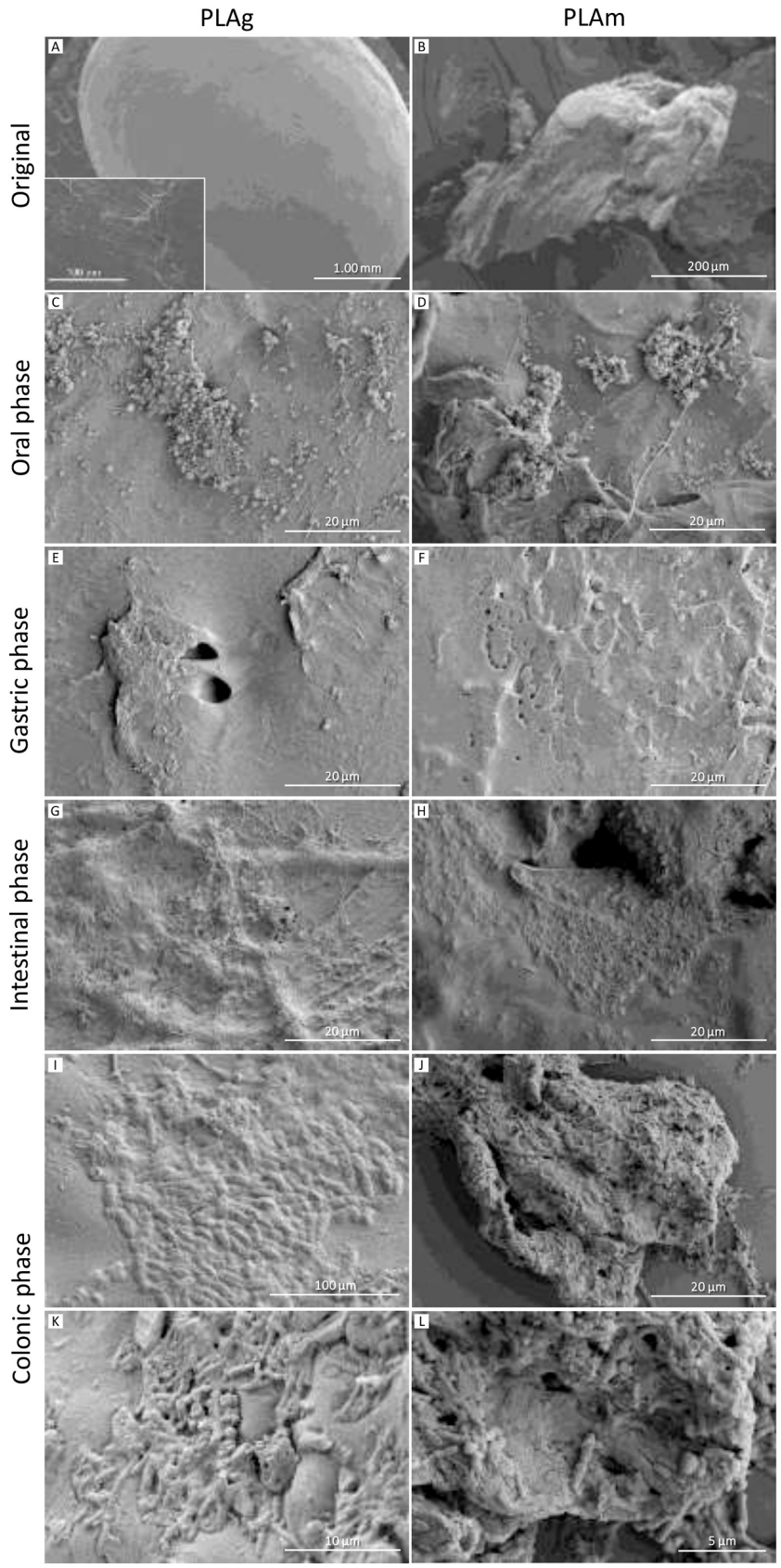

Fig. 2. Field emission scanning electron micrographs (FESEM) of the surface of polylactic acid (PLAg, millimetric, left, and PLAm, micrometric, right) before (A-B) and after every step of digestion (oral, C-D; gastric, *E*-F; intestinal, G-H; and colonic, I-J, with the corresponding magnifications in K-L, phases).

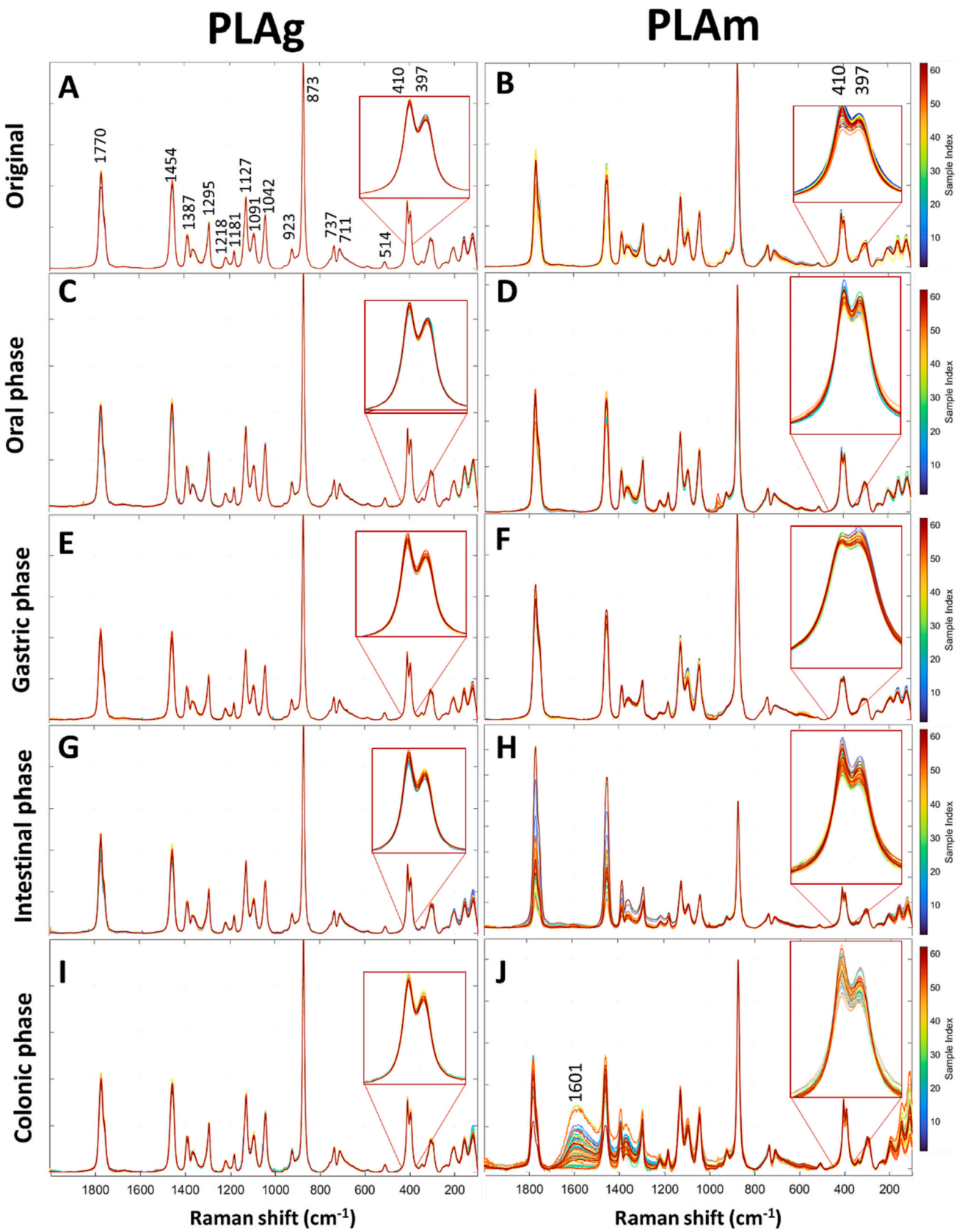

Fig. 3. Raman spectra at 60 representative points of PLA (PLAg, millimetric, left, and PLAm, micrometric, right) in the original state (A-B), after oral (C—D), gastric (E-F), intestinal (G-H) and colonic (I-J) phases. Spectra normalized to the Raman band at 873 cm^{-1}.

no clear extended alteration of PLAg, in agreement with the localized nature of the surface alterations observed by FESEM. In contrast, incipient inhomogeneity is apparent in PLAm after gastric stage (Fig. 3F), in line with the incipient modifications discovered by FESEM. The Raman bands at 1218, 1181, and 1091 cm^{-1}, associated with O-C-O ester group vibration modes, and Raman band at 514 cm^{-1}, associated with crystalline PLA, show some intensity variability, along with the Raman bands near 1770 and 1454 cm^{-1}, associated with the carbonyl group and with the methyl in-plane asymmetric wagging of the ester group (Qin and Kean, 1998). These inhomogeneities are extensive after the small intestine phase (Fig. 3H), particularly in the carbonyl region, near 1770 cm^{-1}, and the methyl modes in the 1460–1200 cm^{-1} window.

Some incipient amorphous carbon deposits are already apparent (the broad feature in the 1250–1650 cm^{-1} window, which area is presented below as A_{1601}); these are clear and extensively present on PLAm after colonic fermentation (Fig. 3J). The intensity of amorphous carbon deposits changes significantly from one spectrum to another, that is, from one spot to another during the mapping of these samples. This may be associated with differences in the amount of amorphous carbon residue deposited at different points. This is analyzed by confocal depth Raman profile measurements (Fig. 5).

Several Raman modes are associated with the crystallinity degree of PLA (amorphous, semicrystalline, or crystalline); their relative intensities are used as descriptors of crystallinity variations. The band at ca. 397 cm^{-1} is associated with amorphous PLA structures, whereas the band at ca. 409 cm^{-1} is associated with crystalline PLA (Smith et al., 2001). Thus, the 397/410 intensity ratio in Fig. 4A is related to the degree of amorphicity. This parameter indicates that the PLAm series is more amorphous and has a broader crystallinity distribution than PLAg. In addition, PLAm crystallinity passes through a relatively low gastric phase during the simulated human digestion. A similar result is obtained with the analysis of the Raman modes near 923 and 711 cm^{-1}, which are absent in amorphous samples but grow in semicrystalline PLA (Vano-Herrera and Vogt, 2017). The relative intensities of 923 and 711 cm^{-1} Raman bands vs. that of 873 cm^{-1} internal reference, illustrated in Fig. 4B and C, respectively, show lower semi crystallinity in PLAm vs. PLAg series, and a local minimum of semi crystallinity for PLAm after the gastric phase. The Raman band near 1770 cm^{-1} is a complex overlap of PLA carbonyl group signals with different degrees of crystallinity (Kister et al., 1998). The relative area of the 1770 cm^{-1} band vs. internal reference at 873 cm^{-1} is not significantly different between and within PLAg and PLAm samples, but the higher dispersion of values in PLAm illustrates a broader distribution of states, in agreement with the rest of descriptors.

The higher degradation of PLAm regarding PLAg would be associated with its higher surface-to-volume exposure, which is fostered by the textural features generated during cryomilling. Because PLAm series were more sensitive to digestion-induced alterations than PLAg, a confocal Raman depth profile analysis was performed on representative PLAm samples, after oral and intestine stages, to assess if the observed phenomena are essentially surface-related -as expected- or may reach the bulk. However, whereas PLAg is more stable than PLAm, FESEM demonstrated the formation of holes at its surface (Fig. 2E), and the most intense variations of PLA Raman modes are associated with the presence of amorphous carbonaceous deposits on the surface (Fig. 3J), which would suggest that the structural modifications are at the PLA-carbon deposit interface region. Therefore, we also explored PLAg with confocal Raman microscopy in search of representative chemical modifications on the microplastic surface. Given the transparency of PLA, the ca. The 1 μm confocal volume cannot prevent the signal from areas outside the confocal region. Fig. 5 illustrates the Raman depth profiles of digested PLAm, the Raman area of the representative Raman band at 1601 cm^{-1} (A_{1601}) and the amorphicity descriptors as a function of the distance above (positive Z values) or below (negative) the surface. Oral PLAm shows little change with depth scan and no presence of amorphous carbonaceous species in the range from 4 μm inside the particles (Z = −4) up to 4 μm above the surface (Z = 4), except for a couple of spectra (Fig. 5A, B). The semi crystallinity indicators I_{711}/I_{873} and I_{923}/I_{783} reveal no significant variability (Fig. 5D), and there is also no increase in amorphous PLA, associated with the intensity ratio of the 397/410 cm^{-1} Raman bands (Fig. 5C). The scenario is different after gastric digestion (Fig. 5E), where amorphous carbon deposits are apparent; the normalized Raman area of carbonaceous species is low inside PLAm particles, but increasingly important above the surface (Fig. 5F). Semi crystallinity has hardly any fluctuation in the regions where carbon deposits are present, with few spots showing higher semi crystallinity, but without a clear trend (Fig. 5H). The Raman spectra show no development of amorphous PLA, as measured by the I_{397}/I_{410} ratio (Fig. 5G). The stage of the small intestine resulted in the most apparent modifications, both in the structure of PLAm and in the accumulation of carbon species (Fig. 5I). The area of the representative Raman band near 1601 cm^{-1} (A_{1601}) is the highest in the samples studied and, again, much more intense above the PLAm surface than inside the particle (Fig. 5J). The 1601 cm^{-1} band grows in parallel with several weaker bands in the

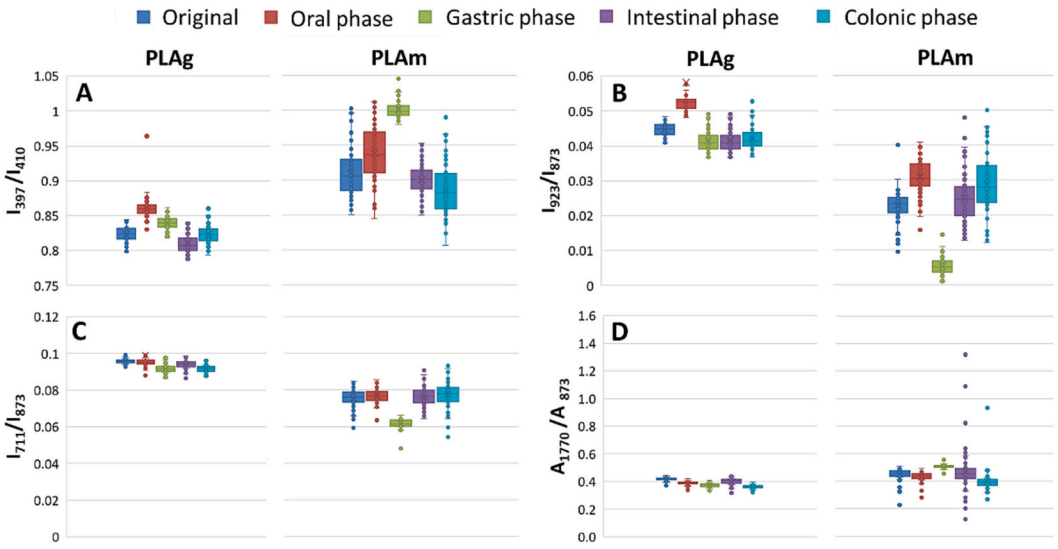

Fig. 4. Raman descriptors for PLA amorphicity based on the relative intensities or areas of the Raman bands at 397 vs. 410 cm^{-1} (A), at 923 vs. 873 cm^{-1} (B), at 711 vs. 873 cm^{-1} (C), and at 1770 vs. 873 cm^{-1} (D).

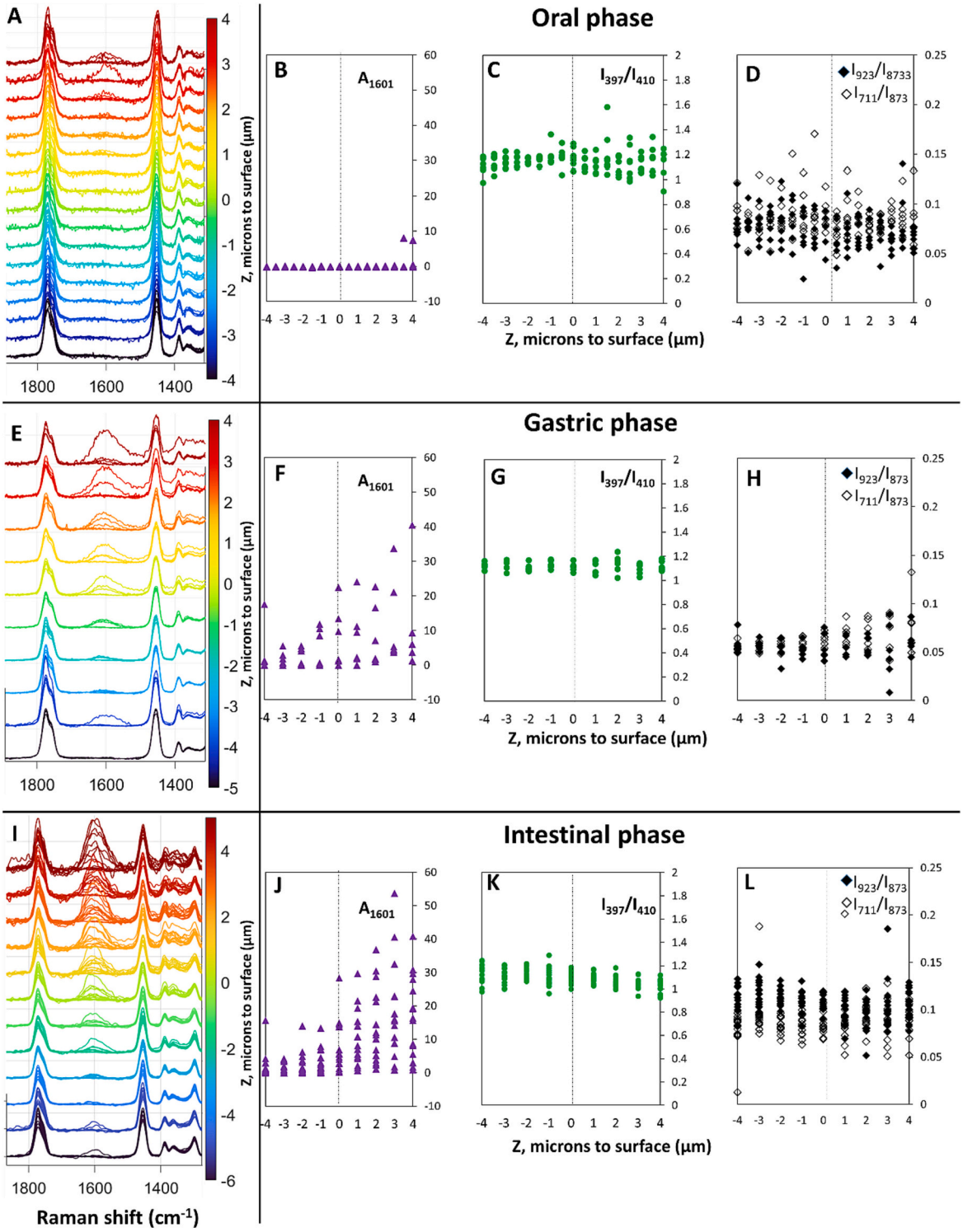

Fig. 5. Depth profile Raman evaluation for PLAm after oral phase (A-D), gastric phase (E-H), and intestinal digestion (I—K). A, E, I: Raman spectra as a function of penetration depth. B, F, J: area of the 1601 cm^{-1} Raman band of amorphous carbon deposits. C, G, K: relative intensity of the Raman band at 397 vs. 410 cm^{-1}, amorphicity indicator. D, H, L: relative intensities of the Raman bands at 923 and 711 cm^{-1} regarding the reference band at 873 cm^{-1}, semi-crystallinity indicators. Spectra normalized to the Raman band at 873 cm^{-1}.

2300–2100, 2020–1950, 1850–1700, 1500–1300, 1300–1100, 1000–850, and 800–700 cm^{-1} regions, associated with biofilm (Cialla-May et al., 2022; Horiue et al., 2020; Pezzotti, 2021). PLAm particles after small intestine digestion exhibit much higher semi crystallinity (I_{873}/I_{711} and I_{873}/I_{923} in Fig. 5L) than after gastric or oral phases, concentrated near the surface, associated with the presence of carbonaceous deposits. There is no evolution to an amorphous PLA phase (I_{397}/I_{410} ratio in Fig. 5K). Therefore, carbonaceous deposits appear associated with a loss of crystallinity at the surface toward semicrystalline PLA; there is no signal of further deconstruction toward amorphous domains in any digestion stage.

3.3. Impact of PLA digestion on the colonic microbiota

As a first approach, the effect of PLA MPs on the colonic microbiota was evaluated by plate counting in nine culture media (Table 1). From a microbiological viewpoint and because of plate counting limitations, differences were only considered if they were statistically significant and with a Δlog (CFU/mL) ≥ 1 (Gil-Sánchez et al., 2018). Compared to the control, Volunteer 1 showed differences at 0 h in the counts of lactic acid bacteria for PLAg and in *Staphylococcus* spp. for PLAm. At 24 h, there were differences for both PLAm and PLAg in members of the *Enterobacteriaceae* family, with lower and higher levels compared to the control, respectively. At 72 h, PLAg showed higher levels in lactic acid bacteria counts. However, no differences were found regarding the control in any sample/time from volunteers 2 and 3.

16S rRNA gene-based sequencing analysis and subsequent study of microbial diversity and composition were conducted. Regarding biodiversity, significant differences were found in the *alpha*-diversity indexes (Shannon and Simpson) and *beta* diversity, depending on the volunteer (Table S1 and Fig. S1). For Volunteer 1, PLAm led to a decrease in Shannon and Simpson *alpha*-diversity indexes at 48 h, the same result was at 24 h with PLAg and at 24 h and 48 h with PLAm in Volunteer 3. Regarding beta diversity, changes on structure of microbial communities over time for Volunteer 1 were similar for the three conditions, except for PLAm at 48 h. For volunteers 2 and 3, the conditions of PLAm and PLAg showed a different composition between them and the control at 24 h, also different at 48 h for PLAg in Volunteer 2 and at 72 h for PLAm in Volunteer 3. Regarding phylo-genetic analysis, results revealed differences in the relative proportions of some taxa after PLA MP

Table 1
Evolution of the main microbial groups with colonic fermentation time evaluated by plate counting in nine culture media. Lowercase letters denote statistically significant differences between colonic fermentations within bacterial group. Differences regarding the control that are statistically significant ($p < 0.05$) and with Δlog (CFU/mL) ≥ 1 are marked in gray.

VOLUNTEER 1

Time (h)	Sample	Total aerobic	Total anaerobic	*Enterobacteriaceae*	*Enterococcus* spp.	Lactic acid bacteria	*Clostridium* spp.	*Staphylococcus* spp.	Intestinal *Lactobacillus*	*Bifidobacterium* spp.
0	PLAm	4.33 ± 0.17 ^{f}	7.49 ± 0.02 ^{b}	3.90 ± 0.03 ^{de}	4.33 ± 0.03 ^{f}	5.14 ± 0.21 ^{de}	4.33 ± 0.10 ^{bc}	5.34 ± 0.06 ^{c}	4.30 ± 0.04 ^{b}	6.64 ± 0.57 ^{d}
	PLAg	4.91 ± 0.12 ^{f}	6.96 ± 0.59 ^{b}	4.63 ± 0.03 ^{c}	4.14 ± 0.02 ^{g}	6.23 ± 0.40 ^{c}	4.06 ± 0.06 ^{c}	4.46 ± 0.11 ^{d}	4.05 ± 0.02 ^{c}	6.49 ± 0.50 ^{d}
	Control	5.00 ± 0.04 ^{f}	7.50 ± 0.24 ^{b}	4.50 ± 0.12 ^{cd}	4.22 ± 0.04 ^{fg}	4.95 ± 0.20 ^{e}	4.37 ± 0.03 ^{b}	4.27 ± 0.08 ^{d}	4.02 ± 0.16 ^{c}	6.98 ± 0.05 ^{d}
24	PLAm	5.94 ± 0.12 ^{cde}	8.93 ± 0.08 ^{a}	3.69 ± 0.09 ^{e}	5.68 ± 0.06 ^{d}	7.66 ± 0.09 ^{a}	7.32 ± 0.04 ^{a}	5.54 ± 0.03 ^{bc}	5.06 ± 0.06 ^{a}	7.36 ± 0.07 ^{bc}
	PLAg	7.07 ± 0.13 ^{a}	9.01 ± 0.17 ^{a}	6.74 ± 0.08 ^{a}	6.65 ± 0.04 ^{a}	7.22 ± 0.14 ^{ab}	7.33 ± 0.05 ^{a}	6.35 ± 0.07 ^{ab}	5.15 ± 0.10 ^{a}	7.22 ± 0.02 ^{cd}
	Control	6.22 ± 0.10 ^{cd}	9.11 ± 0.15 ^{a}	4.98 ± 0.05 ^{b}	6.17 ± 0.02 ^{b}	7.34 ± 0.12 ^{ab}	7.24 ± 0.06 ^{a}	6.02 ± 0.08 ^{b}	4.92 ± 0.08 ^{a}	7.18 ± 0.07 ^{cd}
48	PLAm	6.61 ± 0.05 ^{ab}	8.94 ± 0.03 ^{a}	2.69 ± 0.36 ^{f}	6.5 ± 0.11 ^{ab}	7.01 ± 0.11 ^{b}	7.41 ± 0.03 ^{a}	6.44 ± 0.09 ^{a}	4.38 ± 0.04 ^{b}	7.67 ± 0.06 ^{ab}
	PLAg	6.11 ± 0.00 ^{cd}	8.75 ± 0.05 ^{ab}	2.76 ± 0.15 ^{f}	5.49 ± 0.11 ^{de}	7.29 ± 0.07 ^{ab}	7.33 ± 0.07 ^{a}	5.56 ± 0.02 ^{bc}	4.49 ± 0.05 ^{b}	7.33 ± 0.05 ^{c}
	Control	6.27 ± 0.08 ^{cd}	8.62 ± 0.25 ^{ab}	2.91 ± 0.13 ^{f}	6.16 ± 0.08 ^{bc}	6.27 ± 0.07 ^{c}	7.25 ± 0.10 ^{a}	5.72 ± 0.05 ^{b}	4.04 ± 0.13 ^{c}	7.25 ± 0.08 ^{cd}
72	PLAm	5.42 ± 0.02 ^{e}	8.48 ± 0.06 ^{ab}	3.28 ± 0.06 ^{f}	5.34 ± 0.04 ^{e}	6.19 ± 0.08 ^{c}	7.05 ± 0.19 ^{a}	5.78 ± 0.30 ^{b}	3.08 ± 0.13 ^{d}	8.15 ± 0.14 ^{a}
	PLAg	6.39 ± 0.06 ^{bc}	8.39 ± 0.04 ^{ab}	2.20 ± 0.35 ^{f}	6.37 ± 0.21 ^{ab}	6.43 ± 0.06 ^{c}	7.12 ± 0.07 ^{a}	6.39 ± 0.15 ^{ab}	3.19 ± 0.06 ^{d}	7.59 ± 0.11 ^{abc}
	Control	5.87 ± 0.11 ^{de}	8.39 ± 0.01 ^{ab}	2.60 ± 0.30 ^{f}	5.78 ± 0.02 ^{cd}	5.94 ± 0.12 ^{cd}	7.08 ± 0.15 ^{a}	5.94 ± 0.21 ^{b}	2.53 ± 0.21 ^{d}	7.92 ± 0.08 ^{a}

VOLUNTEER 2

Time (h)	Sample	Total aerobic	Total anaerobic	*Enterobacteriaceae*	*Enterococcus* spp.	Lactic acid bacteria	*Clostridium* spp.	*Staphylococcus* spp.	Intestinal *Lactobacillus*	*Bifidobacterium* spp.
0	PLAm	6.09 ± 0.09 ^{d}	8.27 ± 0.06 ^{b}	5.50 ± 0.04 ^{b}	5.73 ± 0.02 ^{c}	6.98 ± 0.18 ^{bc}	7.71 ± 0.05 ^{c}	6.03 ± 0.01 ^{c}	5.02 ± 0.06 ^{b}	7.91 ± 0.12 ^{bc}
	PLAg	5.94 ± 0.03 ^{d}	8.28 ± 0.07 ^{b}	5.52 ± 0.03 ^{b}	5.69 ± 0.07 ^{c}	7.10 ± 0.11 ^{ab}	7.94 ± 0.06 ^{bc}	5.92 ± 0.03 ^{c}	5.08 ± 0.07 ^{b}	7.98 ± 0.07 ^{b}
	Control	6.05 ± 0.08 ^{d}	8.31 ± 0.05 ^{b}	5.51 ± 0.03 ^{b}	5.72 ± 0.04 ^{c}	7.19 ± 0.02 ^{ab}	8.02 ± 0.06 ^{b}	5.91 ± 0.03 ^{c}	5.33 ± 0.06 ^{ab}	7.99 ± 0.13 ^{ab}
24	PLAm	7.29 ± 0.05 ^{a}	9.15 ± 0.03 ^{a}	6.68 ± 0.05 ^{a}	6.96 ± 0.03 ^{a}	7.49 ± 0.07 ^{a}	8.64 ± 0.01 ^{a}	7.09 ± 0.02 ^{a}	5.41 ± 0.05 ^{a}	8.39 ± 0.04 ^{a}
	PLAg	7.23 ± 0.04 ^{ab}	9.08 ± 0.04 ^{a}	6.62 ± 0.04 ^{a}	6.90 ± 0.02 ^{a}	7.45 ± 0.04 ^{a}	8.54 ± 0.02 ^{a}	7.13 ± 0.06 ^{a}	5.32 ± 0.02 ^{ab}	8.28 ± 0.07 ^{ab}
	Control	7.30 ± 0.04 ^{a}	9.14 ± 0.02 ^{a}	6.72 ± 0.03 ^{a}	6.93 ± 0.04 ^{a}	7.31 ± 0.04 ^{ab}	8.65 ± 0.04 ^{a}	7.06 ± 0.08 ^{a}	5.28 ± 0.06 ^{ab}	8.44 ± 0.02 ^{a}
48	PLAm	6.83 ± 0.26 ^{bc}	8.54 ± 0.06 ^{b}	4.87 ± 0.04 ^{c}	6.90 ± 0.00 ^{a}	7.08 ± 0.07 ^{b}	7.59 ± 0.04 ^{cd}	6.92 ± 0.15 ^{ab}	3.11 ± 0.10 ^{d}	8.40 ± 0.03 ^{a}
	PLAg	7.10 ± 0.07 ^{ab}	8.48 ± 0.06 ^{b}	4.74 ± 0.02 ^{c}	6.95 ± 0.05 ^{a}	7.20 ± 0.10 ^{ab}	7.77 ± 0.04 ^{bc}	7.10 ± 0.18 ^{a}	3.47 ± 0.08 ^{d}	8.25 ± 0.04 ^{ab}
	Control	7.14 ± 0.09 ^{ab}	8.51 ± 0.13 ^{b}	4.75 ± 0.15 ^{c}	6.95 ± 0.17 ^{a}	7.05 ± 0.13 ^{b}	7.99 ± 0.05 ^{b}	7.01 ± 0.11 ^{ab}	4.04 ± 0.12 ^{c}	8.29 ± 0.08 ^{ab}
72	PLAm	6.60 ± 0.09 ^{c}	8.28 ± 0.02 ^{b}	4.53 ± 0.03 ^{d}	6.51 ± 0.08 ^{b}	5.77 ± 0.07 ^{e}	7.47 ± 0.05 ^{d}	6.61 ± 0.07 ^{b}	2.00 ± 0.00 ^{e}	7.44 ± 0.01 ^{c}
	PLAg	6.80 ± 0.17 ^{bc}	8.30 ± 0.07 ^{b}	4.24 ± 0.05 ^{e}	6.63 ± 0.03 ^{b}	6.28 ± 0.06 ^{cd}	7.55 ± 0.02 ^{cd}	6.94 ± 0.03 ^{ab}	1.43 ± 1.25 ^{e}	7.56 ± 0.07 ^{c}
	Control	6.97 ± 0.07 ^{bc}	8.49 ± 0.04 ^{b}	4.10 ± 0.07 ^{e}	6.60 ± 0.09 ^{b}	5.85 ± 0.15 ^{de}	7.96 ± 0.09 ^{bc}	6.67 ± 0.06 ^{b}	2.59 ± 0.26 ^{de}	7.90 ± 0.00 ^{bc}

VOLUNTEER 3

Time (h)	Sample	Total aerobic	Total anaerobic	*Enterobacteriaceae*	*Enterococcus* spp.	Lactic acid bacteria	*Clostridium* spp.	*Staphylococcus* spp.	Intestinal *Lactobacillus*	*Bifidobacterium* spp.
0	PLAm	5.82 ± 0.11 ^{c}	8.07 ± 0.04 ^{c}	5.74 ± 0.04 ^{bc}	5.14 ± 0.13 ^{de}	7.09 ± 0.02 ^{ab}	7.46 ± 0.03 ^{e}	5.62 ± 0.10 ^{d}	0.00 ± 0.00	7.46 ± 0.05 ^{c}
	PLAg	6.27 ± 0.07 ^{c}	8.18 ± 0.04 ^{c}	5.94 ± 0.03 ^{a}	5.05 ± 0.08 ^{de}	7.35 ± 0.05 ^{a}	7.54 ± 0.04 ^{de}	5.72 ± 0.03 ^{d}	0.00 ± 0.00	7.56 ± 0.05 ^{c}
	Control	5.88 ± 0.09 ^{c}	8.14 ± 0.08 ^{c}	5.65 ± 0.04 ^{c}	5.28 ± 0.04 ^{d}	7.21 ± 0.04 ^{a}	7.48 ± 0.03 ^{e}	5.58 ± 0.03 ^{d}	0.00 ± 0.00	7.51 ± 0.02 ^{c}
24	PLAm	7.32 ± 0.13 ^{a}	9.05 ± 0.08 ^{a}	5.60 ± 0.30 ^{c}	7.13 ± 0.08 ^{a}	6.95 ± 0.05 ^{b}	8.51 ± 0.07 ^{a}	7.33 ± 0.02 ^{a}	0.00 ± 0.00	8.45 ± 0.04 ^{a}
	PLAg	7.54 ± 0.12 ^{a}	8.70 ± 0.02 ^{ab}	5.91 ± 0.03 ^{ab}	7.24 ± 0.11 ^{a}	7.38 ± 0.07 ^{a}	8.36 ± 0.02 ^{ab}	7.34 ± 0.02 ^{a}	0.00 ± 0.00	8.43 ± 0.06 ^{a}
	Control	7.41 ± 0.06 ^{a}	8.61 ± 0.04 ^{b}	5.84 ± 0.06 ^{abc}	7.29 ± 0.06 ^{a}	7.11 ± 0.10 ^{ab}	8.49 ± 0.04 ^{a}	7.41 ± 0.04 ^{a}	0.00 ± 0.00	8.44 ± 0.02 ^{a}
48	PLAm	7.29 ± 0.03 ^{a}	8.50 ± 0.06 ^{b}	2.99 ± 0.11 ^{ef}	6.21 ± 0.09 ^{b}	3.49 ± 0.05 ^{c}	8.22 ± 0.05 ^{b}	6.58 ± 0.02 ^{c}	0.00 ± 0.00	7.92 ± 0.06 ^{b}
	PLAg	7.42 ± 0.07 ^{a}	8.71 ± 0.02 ^{ab}	3.03 ± 0.12 ^{def}	6.18 ± 0.03 ^{b}	3.54 ± 0.06 ^{c}	8.53 ± 0.04 ^{a}	7.12 ± 0.07 ^{a}	0.00 ± 0.00	8.23 ± 0.09 ^{ab}
	Control	7.40 ± 0.03 ^{a}	8.59 ± 0.05 ^{b}	2.46 ± 0.15 ^{f}	6.11 ± 0.13 ^{bc}	3.54 ± 0.10 ^{c}	8.36 ± 0.05 ^{ab}	6.70 ± 0.03 ^{b}	0.00 ± 0.00	8.29 ± 0.03 ^{a}
72	PLAm	6.65 ± 0.04 ^{b}	7.55 ± 0.06 ^{d}	3.38 ± 0.07 ^{de}	4.86 ± 0.07 ^{e}	3.37 ± 0.08 ^{c}	7.66 ± 0.02 ^{cd}	3.91 ± 0.13 ^{e}	0.00 ± 0.00	6.46 ± 0.05 ^{d}
	PLAg	7.13 ± 0.11 ^{ab}	8.04 ± 0.07 ^{c}	3.52 ± 0.09 ^{d}	5.48 ± 0.04 ^{c}	3.53 ± 0.07 ^{c}	7.90 ± 0.05 ^{c}	4.25 ± 0.07 ^{e}	0.00 ± 0.00	7.22 ± 0.09 ^{c}
	Control	6.83 ± 0.02 ^{b}	7.54 ± 0.06 ^{d}	2.83 ± 0.13 ^{ef}	4.87 ± 0.24 ^{de}	3.40 ± 0.13 ^{c}	7.08 ± 0.11 ^{e}	3.84 ± 0.10 ^{e}	0.00 ± 0.00	7.26 ± 0.08 ^{c}

fermentation. At the phylum level (Table 2), and regarding Volunteer 1, after PLAm fermentation, there was an increase in Proteobacteria members at 48 h and a decrease in Actinobacteriota at 72 h, compared to the control. For Volunteer 2, PLAg showed a reduction in Bacteroidota levels at 24 h, but increased proportions of Desulfobacteria at 24, 48, and 72 h. Furthermore, although the relative abundance of Actinobacteriota at 0 h was higher for PLAg than for the control, no further differences were found later. After the colonic fermentation of the smaller PLAm MPs, only the abundance of Desulfobacterota increased at 24 h. Considering Volunteer 3, Bacteroidota proportions increased in PLAm samples at 24, 48, and 72 h. Proteobacteria proportions were lower than the control for PLAg at 24 h, but revealed higher levels at 72 h for PLAm, whereas Firmicutes decreased at 48 and 72 h. However, the initial abundance of Actinobacteria was lower for both PLAg and PLAm compared to the control, which could be related to the heterogeneous nature of the sample and associated potential technical differences in the inoculum of the sample.

Microbiota analysis at the genus level also showed differences between volunteers (Table S2). For Volunteer 1, PLAm showed an increase in the relative abundance of members of the UCG-002 and UCG-003 genera at 48 h, and *Bacteroides, Megasphaera, Desulfovibrio, Clostridium* sensu stricto 1, and *Tyzzerella* at 72 h. Furthermore, PLAm MPs fermentation promoted a decrease in the abundance of *Oscillospira* and *Lachnospiraceae* UCG-010 members at 24 h; *Faecalibacterium, Catenibacterium*, *Tyzzerella,* and *Allisonella* at 48 h; *Slackia* at 48 and 72 h; and *Senegalimassilia* and *Veillonella* at 72 h. The higher proportion of *Bacillus* for the PLAm condition is also noticeable at 0 h, although this difference is not maintained over time. However, PLAg increased UCG-003 at 24 and 72 h, *Prevotella* and *Desulfovibrio* at 48 h, *Clostridium* senso stricto 1 at 48 and 72 h, and *Veillonella* at 72 h. On the contrary, the levels of *Faecalibaterium, Parabacteroides,* and *Erysipelotrichaceae* UCG-003 and *Allisonella* at 48 h and *Slackia* and *Oscillospira* levels at 72 h decreased. Considering Volunteer 2, there were several differences at 0 h. *Collinsella* and *Desulfovibrio* were more abundant in PLAg and PLAm than in the control, whereas there was less abundance of *Parabacteroides* and *Odoribacter* in PLAg and PLAm and *Escherichia/Shigella* in PLAg compared to the control. For longer colonic fermentation times, PLAm increased *Collinsella* and *Bilophila* at 24 h, and decreased *Bacteroides, Lachnospiraceae* UCG-010 and *Odoribacter* at 24 h; *Parabacteroides* at 24 and 72 h; *Escherichia/Shigella* and *Lachnospiraceae* UCG-010 at 24, 48, and 72 h; *Oscillibacter, Desulfovibrio,* and *Colidextribacter* at 48 h; *Barnesiella* at 48 and 72 h; and *Lachnospiraceae* ND3007 group and *Flavonifractor* at 72 h. In the case of PLAg, an increase was observed in members of *Faecalibacterium* at 24 h; *Prevotellaceae* NK3B31 group at 48 h; *Collinsella* and *Bifidobacterium* at 24 and 48 h; and *Bilophila* at 24, 48, and 72 h. Furthermore, PLAg decreased *Bacteroides* at 24 h, *Escherichia/Shigella* at 24 and 72 h, *Parabacteroides* and *Odoribacter* at 24, 48, and 72 h, *Barnesiella* at 48 h, and *Lachnospiracea*e ND3007 group at 72 h. Finally, the results of Volunteer 3 differed from those of the other volunteers. At 0 h, the proportion of *Adlercreutzia* was lower in PLAg and PLAm than in the control. PLAm fermentation increased the relative abundance of *Bacteroides* and *Parabacteroides* at 24, 48, and 72 h, *Slackia* at 48 h and *Parasutterella* at 72 h, but decreased *Megasphaera* at 24 and 72 h; *Christensenellaceae* R-7 at 24, 48, and 72 h; *Parasutterella* at 24 h; and UCG-002 at 72 h. However, in PLAg samples, *Megasphaera, Slackia, Alistipes,* and *Lachnoclostridium* increased at 24 h; however, a decrease was observed in *Oscillibacter* at 24 and 48 h, as well as in the *Subdoligranulum*, *Parasutterella,* and *Christensenellaceae* R-7 group at 24 h. Furthermore, at 0 h there were differences compared to the control, as *Bacteroides* relative abundance was higher, but *Lachnospira*, *Senegalimassilia,* and *Christensenellaceae* R-7 group relative proportions were lower for both types of MPs.

When comparing the three volunteers, there was few statistically significant differences in at least two of them. The relative abundance in *Bacteroides* showed an increase at 72 h after PLAm treatment in volunteers 1 and 3, and, although it was not statistically significant, the same trend was observed in Volunteer 2. Furthermore, PLAg decreased the relative abundance of *Parabacteroides* at 48 h in volunteers 1 and 2, but this effect was not detected in Volunteer 3. Moreover, *Lachnospiraceae* UCG-010 decreased at 24 h in the presence of PLAm in volunteers 1 and 2.

To investigate the colonic metabolism, SCFA and lactate were analyzed (Tables S3 and S4). In Volunteer 1, the concentration of acetic and total SCFA at 0 h was slightly lower in PLAg than in PLAm and

Table 2
Phylum level. Mean relative abundances (%) and standard deviation for the three volunteers at different colonic fermentation times. Only phyla with a mean relative abundance >0.5 % were considered. Statistical differences (p-adjust <0.05) regarding the control and PLAg/PLAm for each volunteer are highlighted (gray) as well as those common between volunteers (orange).

Volunteer 1												
Time (h)	0			24			48			72		
Sample	Control	PLAg	PLAm	Control	PLAg	PLAm	Control	PLAg	PLAm	Control	PLAg	PLAm
Bacteroidota	52.26 ± 2.71	48.83 ± 5.07	52.47 ± 1.40	49.66 ± 2.88	38.05 ± 1.93	53.00 ± 1.39	38.09 ± 1.19	39.25 ± 1.82	37.99 ± 2.76	28.15 ± 1.95	31.04 ± 4.08	35.59 ± 0.53
Actinobacteriota	0.61 ± 0.14	0.76 ± 0.29	0.58 ± 0.11	2.19 ± 0.17	4.38 ± 1.02	1.24 ± 0.27	4.47 ± 0.58	2.94 ± 0.27	2.62 ± 0.66	5.42 ± 0.28	3.65 ± 1.66	1.21 ± 0.07
Proteobacteria	6.21 ± 0.40	6.34 ± 2.22	5.40 ± 0.07	12.22 ± 0.86	15.08 ± 1.01	10.61 ± 0.17	9.85 ± 0.56	10.22 ± 0.04	14.22 ± 1.68	13.95 ± 0.86	13.13 ± 2.35	11.98 ± 1.03
Firmicutes	38.72 ± 1.80	41.80 ± 2.53	39.90 ± 1.17	33.14 ± 1.41	39.00 ± 2.18	31.90 ± 0.47	46.06 ± 1.45	44.57 ± 1.52	41.95 ± 0.85	47.86 ± 1.26	48.85 ± 1.18	45.93 ± 1.42
Desulfobacterota	2.17 ± 0.40	2.24 ± 0.70	1.57 ± 0.03	2.59 ± 0.63	3.46 ± 0.51	3.02 ± 0.57	1.49 ± 0.18	2.97 ± 0.08	3.07 ± 0.92	4.44 ± 1.02	3.29 ± 1.19	5.14 ± 0.76
Volunteer 2												
Time (h)	0			24			48			72		
Sample	Control	PLAg	PLAm	Control	PLAg	PLAm	Control	PLAg	PLAm	Control	PLAg	PLAm
Bacteroidota	41.51 ± 1.32	38.95 ± 1.11	41.31 ± 1.29	49.80 ± 0.92	42.26 ± 0.44	45.58 ± 1.05	45.85 ± 0.87	40.41 ± 0.39	48.83 ± 2.82	41.71 ± 0.64	36.39 ± 0.72	41.29 ± 0.75
Actinobacteriota	1.12 ± 0.16	2.49 ± 0.23	2.42 ± 0.39	2.97 ± 0.20	6.73 ± 0.31	5.30 ± 0.74	3.05 ± 0.15	6.30 ± 0.57	2.81 ± 0.76	4.30 ± 0.35	7.19 ± 0.82	4.98 ± 0.15
Proteobacteria	15.33 ± 0.79	14.05 ± 0.45	12.39 ± 1.04	10.73 ± 0.44	10.68 ± 0.37	10.57 ± 0.21	10.26 ± 0.07	10.34 ± 0.25	8.02 ± 0.48	9.04 ± 0.43	9.58 ± 0.39	7.68 ± 0.55
Firmicutes	36.86 ± 0.71	38.76 ± 1.06	37.81 ± 0.48	31.99 ± 1.14	34.28 ± 0.63	32.62 ± 1.26	35.69 ± 0.70	35.96 ± 0.64	36.29 ± 2.22	39.77 ± 0.48	40.27 ± 0.59	41.97 ± 1.35
Desulfobacterota	3.67 ± 0.10	4.67 ± 0.23	5.29 ± 0.49	4.30 ± 0.29	5.74 ± 0.08	5.60 ± 0.23	4.85 ± 0.14	6.58 ± 0.03	3.62 ± 0.20	4.71 ± 0.25	6.18 ± 0.08	3.68 ± 0.36
Verrucomicrobiota	1.49 ± 0.18	1.07 ± 0.08	0.75 ± 0.16	0.14 ± 0.03	0.26 ± 0.05	0.17 ± 0.02	0.25 ± 0.02	0.38 ± 0.02	0.42 ± 0.06	0.32 ± 0.02	0.36 ± 0.04	0.38 ± 0.02
Volunteer 3												
Time (h)	0			24			48			72		
Sample	Control	PLAg	PLAm	Control	PLAg	PLAm	Control	PLAg	PLAm	Control	PLAg	PLAm
Bacteroidota	39.06 ± 2.66	45.46 ± 0.91	48.63 ± 2.07	37.38 ± 1.69	40.40 ± 0.74	48.41 ± 1.18	34.31 ± 0.65	29.33 ± 10.30	40.60 ± 0.33	33.63 ± 2.43	29.56 ± 0.30	49.87 ± 2.25
Actinobacteriota	7.26 ± 0.79	1.74 ± 0.19	1.82 ± 0.62	14.74 ± 0.81	14.02 ± 0.37	16.41 ± 1.33	15.78 ± 1.46	17.48 ± 3.75	18.38 ± 2.03	11.15 ± 2.57	14.65 ± 0.82	11.61 ± 1.53
Proteobacteria	5.07 ± 0.41	6.42 ± 0.27	6.14 ± 0.38	10.81 ± 0.67	6.21 ± 0.36	8.79 ± 0.67	10.29 ± 1.38	9.76 ± 4.90	9.05 ± 0.58	6.08 ± 0.46	7.58 ± 0.22	11.04 ± 0.20
Firmicutes	46.86 ± 2.22	45.52 ± 0.47	42.61 ± 1.60	34.22 ± 1.90	37.39 ± 0.70	25.03 ± 1.96	37.06 ± 0.87	37.54 ± 6.08	30.28 ± 1.46	46.38 ± 0.87	45.03 ± 0.90	26.21 ± 0.65
Desulfobacterota	1.63 ± 0.03	0.77 ± 0.05	0.72 ± 0.13	2.83 ± 0.26	1.96 ± 0.02	1.36 ± 0.22	2.46 ± 0.33	1.94 ± 1.45	1.66 ± 0.03	2.71 ± 0.30	3.07 ± 0.48	1.26 ± 0.04
Verrucomicrobiota	0.10 ± 0.03	0.06 ± 0.01	0.06 ± 0.01	0.01 ± 0.01	0.01 ± 0.01	0.00 ± 0.00	0.03 ± 0.01	3.94 ± 6.80	0.00 ± 0.01	0.03 ± 0.01	0.03 ± 0.01	0.00 ± 0.00

control. Furthermore, the PLAm sample showed a higher concentration of lactate than the PLAg and control samples at 0 h. However, there were no remarkable differences at other times. Differences between samples in volunteers 2 and 3 were found for neither SCFA nor for lactate.

To evaluate whether some bacterial metabolic pathways and functions could be associated with PLA MPs modification or degradation, a bioinformatic functional prediction analysis from 16S rRNA gene sequencing analysis data was performed, considering samples from the three volunteers together to identify general trends. Results of *Tax4Fun2* functional prediction are shown in supplementary Tables 5 and 6, both at gene/functions and pathways levels at the different fermentations timepoints (Tables S5 and S6). However, only a few pathways and functions were remarkable, highlighting the steroid degradation pathway, related to xenobiotic biodegradation and metabolism, which was more represented in PLAm samples at 48 h than in the control. Regarding specific functions, the results pointed to a higher relative abundance of a sequence assigned to pullulanase activity in PLAg samples at 24 h.

4. Discussion

Due to the complexity of human studies with MPs and ethical restrictions, to date, very few studies have attempted to deepen the potential effects of such particles on the human gastrointestinal tract and human health. As an approximation to face these limitations, some work has investigated the impact of MPs on the colonic microbiota using human gastrointestinal in vitro simulators, such as studies of Huang et al. (2021b) and Fournier et al. (2023a, 2023b), which simulated the microbial colonic fermentation of PE MPs, the latter under infant and adult conditions. However, the previous steps of gastrointestinal digestion were not considered, and these may also alter the properties of MPs' particles, thus leading to different effects on gut and colonic-microbial communities. Therefore, Yan et al. (2022b) and Tamargo et al. (2022) simulated the complete gastrointestinal digestion of PET MPs under dynamic conditions, revealing a negative effect of their ingestion on the colonic microbiota, as well as a possible effect of gastrointestinal digestion and colonic-microbial fermentation processes on these MP particles. The results obtained with PET, a polymer from fossil resources, may not be directly applied to other polymers. This would require further studies. Biodegradable and bioresorbable plastics produced from renewable resources, such as PLA, are entering this arena as a potentially safer and more sustainable performer. To the best of our knowledge, this is the first study on the potential effects of human gastrointestinal digestion of millimetric and micrometric PLA. Furthermore, we consider the impact that digestion and colonic fermentation processes could have on representative bioplastic particles and vice versa, the effects these may have on human gut microbial communities at the compositional and functional level, and therefore on human health. Thus, this study is a necessary step in assessing the possibility of replacing petroleum-derived polymers with reported toxic effects on the health and environment by other polymers that may a priori, be essentially harmless because of their biodegradability, but which have not been evaluated to date.

4.1. Impact of gastrointestinal digestion and microbial colonic fermentation on PLA particles

The FESEM results suggest that the gastrointestinal digestion process changes the morphology of PLA MPs, at least at its surface, and that this modification seems dependent on polymer size. Raman spectra associate these morphological changes with a loss of crystallinity, which is more apparent on PLAm than on PLAg, and is intense after transits of the small intestine and colon. After the gastric phase, the particles showed surface modifications as different pits and pores that appeared in both PLAg and PLAm MPs, which could result from exposure to acid conditions (pH 3). In this sense, previous works have described that simulated human gastric digestion affects the morphology of PS and HDPE MPs, possibly increasing the contact surface area and improving the exposure of surface functional groups, which may affect its interaction with various compounds (Krasucka et al., 2022). Furthermore, Liu et al. (2020) described the relevance of pH in PLA biodegradation, since PLA degraded faster at pH 3 than at neutral pH. However, not only could pH be responsible for this effect but also the type and concentration of gastric enzymes as well as simulation conditions that could affect polymer degradation rate (Agarwal, 2020). After the intestinal phase, no morphological changes were observed apart from a layer of organic matter deposited on the surface, supporting the hypothesis of the formation of a "protein corona" (Stock et al., 2020), related to the deposit of the contents of the intestinal fluid over the MPs, as previously observed with PET MPs (Tamargo et al., 2022). Furthermore, organic matter and a microbial biofilm covered both types of PLA after the colonic fermentation, suggesting colonization of the particles by the colonic microbiota. Some studies have described the adhesion of microorganisms to the surface of MPs due to their ability to deposit nutrients and organic matter on their surface (Oberbeckmann et al., 2015), developing microbial biofilms over time that are significantly different in structure and composition from the surrounding environment (Zettler et al., 2013; Zhang et al., 2021a). In fact, microorganisms have been detected on the surface of PLA MPs after their immersion in the aquatic environment (Bhagwat et al., 2021; Nguyen et al., 2023). In this sense, digestive fluids are rich in organic material, so that, once deposited on the surface of MP, they could favor the adhesion of the colonic microbiota. Raman spectroscopy reveals an incipient build-up of amorphous carbonaceous species at PLA simultaneously with the presence of organic material on the surface of microplastics. Our results are in line with previous works, where a biofilm was detected in PET and PE MPs after the colonic fermentation in the simgi® and the Mucosal Artificial COLon (M-ARCOL) models, respectively (Tamargo et al., 2022; Fournier et al., 2023a, 2023b). In the case of PET MPs, the authors hypothesized that the microbiota adhesion to the surface could have a degrading activity; however, to the best of our knowledge, no microbial proteins or enzymatic activities have been related with MPs metabolism or biodegradation on human gut microbiota. The potential biodegradation or transformation of MPs by gut microbial communities could promote the release of additives or plastic-derived metabolites that could also affect human health with unknown effects (Jiménez-Arroyo et al., 2023). Thus, as a field in its infancy, further investigation is imperative to decipher the impact of these microbial biofilms on PLA MPs structure, the possible transformation and/or biodegradation by human gut microbiome, and potential metabolites produced, as the well as molecular mechanisms responsible.

4.2. Impact of PLA MPs on the colonic microbiota

Our microbiological analyses showed different microbial profiles and trends over time, depending on the volunteer. The human gut microbiome is a complex and diverse ecosystem, with an important interindividual and intraindividual variability depending on different life points, lifestyle, and even days (Vandeputte et al., 2021). Composition varies among healthy individuals, without a clear standard of healthy gut microbiome composition (Fassarella et al., 2021; Huttenhower et al., 2012; Lloyd-Price et al., 2016). The reasons for this diversity remain elusive, although diet, environment, medication, health status, genetics, and early microbial exposure of the host are well-known implicated factors (Huttenhower et al., 2012) that could explain the different microbial profiles at the initial time of the three healthy volunteers of similar age and lifestyle. Furthermore, despite some resilience of the gut microbiome (Fassarella et al., 2021), its response to a challenge/intervention depends on the initial composition and functionality profile of the individual (Klimenko et al., 2022; Schmidt et al., 2018), which could explain the different observed trends. 16S rRNA gene sequencing analysis revealed different microbial profiles between

colonic fermentation of different PLA size series and control condition, highlighting taxons at phylum and genus levels. However, no similar tendencies or positive or negative effects were observed for the three volunteers at any digestion stage, except for the *Bifidobacterium* genus. Few studies have observed the effects of PLA MPs on gut microbiota. Duan et al. (2022) and Yu et al. (2022) reported changes in the relative abundances of some taxa after exposure to PLA MPs in zebrafish and earthworms, respectively. However, to date, no studies have tested the impact of these particles on the human gut. The properties of PLA that have made it suitable for countless medical applications in humans (Li et al., 2022) explains why we have found no changes in most of the microbial communities. These results suggest that, despite the slight modulation observed in microbial communities, the presence of the biodegradable PLA biopolymer on human gut does not exert a negative effect on the human gut microbiome.

Bifidobacterium members showed a tendency to increase their relative proportions in presence of PLAg for the three volunteers, reaching the highest proportion at 24 h for volunteers 1 and 2, and at 48 h for volunteer 3. An explanation could be that *Bifidobacterium* members may have biointeractions with the PLA surface, an effect that may be more pronounced in the case of PLAg due, at least in part, to the smoother surface. In the human body, intestinal epithelial cells are covered by a thick mucus layer, which is crucial for bacterial adhesion and colonization, as well as for interactions between intestinal microbes and host (Harata et al., 2021). This is a process in which *Bifidobacterium* members play a key role due to their ability to produce different molecules such as exopolysaccharides, glycosidases, moonlight factors, extracellular vesicles, or fimbriae, favoring the adhesion and colonization of the intestinal mucosa (Nishiyama et al., 2021) in the absence of an epithelial or mucus layer in colonic fermentation. Moreover, co-existence with other intestinal bacteria can stimulate the production of extracellular vesicles, providing adhesive advantages for *Bifidobacterium* (Nishiyama et al., 2020). However, the increase in *Bifidobacterium* members after PLAg exposure also follows the detection, by functional bioinformatic prediction, of an increase in the relative proportions of a function related to pullulanase activity at 24 h. In this sense, it has been described that members of *Bifidobacterium* use specific polysaccharide-degradation pathways, which vary depending on the strain/species (Nishiyama et al., 2021). Several studies have commented on the pullulanase activity of strains of *Bifidobacterium* in the human gut (Ryan et al., 2006; Yang et al., 2021). Pullulanase, an important debranching enzyme, has been widely used to hydrolyze the α-1,6 glucosidic bonds in starch, amylopectin, pullulan, and related oligosaccharides, enabling complete and efficient conversion of branched polysaccharides into small fermentable sugars during the saccharification process (Hii et al., 2012; Xu et al., 2021). Furthermore, PLA can be in the form of copolymers with pullulan or chitosan (derived from pullulan) to improve its thermoresponsive properties (Basu et al., 2016; Maharana et al., 2015). This pullulanase activity could degrade linkages of polysaccharide branches of PLA copolymers, or because of the polymeric nature of PLA, it could degrade PLA branches into smaller derivative molecules that could provide a carbon source or nutritional advantage to members of *Bifidobacterium,* which explains their relative levels of increase. Members of the *Bifidobacterium* are well known for their positive effects on human health, being one of the most used species/strains as probiotics (Derrien et al., 2022). However, the mechanisms underlying the relationship between this observed increase in *Bifidobacterium* levels and PLAg, as well as potential effects of PLA on gut microbiome and health, are unclear, so we must therefore analyze this effect with caution. Furthermore, this predicted pullulanase activity, with the increase in other functions related to the degradation of xenobiotics detected by bioinformatic functional prediction, could be responsible for the biodegradation and transformation of PLAg and PLAm surfaces observed by FESEM. Raman has detected changes in vibrational modes associated with the O-C-O ester group vibration in the 1000–1220 cm^{-1} window. However, no systematic study has addressed this possibility, so future research should be oriented to test the PLA degrading ability of these putative microbial enzymes and to further investigate the presence of PLA and other MPs degrading activities on the human gut microbiome.

5. Conclusions

In this study, gastrointestinal digestion and colonic fermentation of millimetric and micrometric PLA were investigated for the first time. PLA underwent superficial changes during gastrointestinal digestion. After colonic fermentation, slight alterations were found in the microbial communities of the gut, notably the *Bifidobacterium* genus, which increased for millimetric PLA particles. Microbial biofilms formed on the PLA microplastics surface suggest the colonization of the particles by the colonic microbiota. More studies must verify the observed trends to investigate the possible biodegradation of PLA by the intestinal microbiota and the potential derived metabolites, and to decipher the long-term effects of PLA MPs on human microbiota and health.

CRediT authorship contribution statement

M.A.B., J.F.F. and M.V.M.A. conceived the experiment(s); J.J.R. and J.F.F. produced microplastics and performed FESEM analysis; V.A.-R., R. P. and M.A.B. performed Raman experiments; C.J.-A., A.T., N.M., and M. V.M.A. designed and conducted gastrointestinal simulation experiments and microbiome analysis; C.J.-A., A.T., N.M, and M.V.M.A. analyzed the results. All authors contributed to the writing, editing, and review of the manuscript.

Declaration of competing interest

The authors declare that they have no known competing financial interests or personal relationships that could have appeared to influence the work reported in this paper.

Data availability

No data was used for the research described in the article.

Acknowledgements

This work was supported by the Spanish Ministry of Science and Innovation (Spain), grant number PID2019-108851RB-C21 and the EU H2020 Project "*Plastics Fate and Effects in the human body*" (PlasticsFate) under Grant Agreement no. 95921. The authors thank CSIC Interdisciplinary Thematic Platform for Sustainable Plastics toward a Circular Economy (PTI+ SusPlast).

Appendix A. Supplementary data

Supplementary data to this article can be found online at https://doi.org/10.1016/j.scitotenv.2023.166003.

References

Agarwal, S., 2020. Biodegradable polymers: present opportunities and challenges in providing a microplastic-free environment. Macromol. Chem. Phys. 221 https://doi.org/10.1002/macp.202000017.

Allen, S., Allen, D., Karbalaei, S., Maselli, V., Walker, T.R., 2022. Micro(nano)plastics sources, fate, and effects: what we know after ten years of research. J. Hazard. Mater. Adv. 6, 100057 https://doi.org/10.1016/J.HAZADV.2022.100057.

Athanasiou, K.A., Niederauer, G.G., Agrawal, C.M., 1996. Sterilization, toxicity, biocompatibility and clinical applications of polylactic acid/polyglycolic acid copolymers. Biomaterials 17, 93–102. https://doi.org/10.1016/0142-9612(96)85754-1.

Basu, A., Kunduru, K.R., Doppalapudi, S., Domb, A.J., Khan, W., 2016. Poly(lactic acid) based hydrogels. Adv. Drug Deliv. Rev. 107, 192–205. https://doi.org/10.1016/J.ADDR.2016.07.004.

Bhagwat, G., O'Connor, W., Grainge, I., Palanisami, T., 2021. Understanding the fundamental basis for biofilm formation on plastic surfaces: role of conditioning films. Front. Microbiol. 12 https://doi.org/10.3389/FMICB.2021.687118.
Brodkorb, A., Egger, L., Alminger, M., Alvito, P., Assunção, R., Ballance, S., Bohn, T., et al., 2019. INFOGEST static in vitro simulation of gastrointestinal food digestion. Nat. Protoc. 14, 991–1014. https://doi.org/10.1038/s41596-018-0119-1.
Callahan, Ben J., Sankaran, K., Fukuyama, J.A., McMurdie, P.J., Holmes, S.P., 2016b. Bioconductor workflow for microbiome data analysis: from raw reads to community analyses. F1000Res 5, 1492. https://doi.org/10.12688/f1000research.8986.2.
Callahan, Benjamin J., McMurdie, P.J., Rosen, M.J., Han, A.W., Johnson, A.J.A., Holmes, S.P., 2016a. DADA2: high-resolution sample inference from Illumina amplicon data. Nat. Methods 13, 581–583. https://doi.org/10.1038/nmeth.3869.
Chagas, T.Q., da C. Araújo, A.P., Malafaia, G., 2021a. Biomicroplastics versus conventional microplastics: an insight on the toxicity of these polymers in dragonfly larvae. Sci. Total Environ. 761, 143231 https://doi.org/10.1016/j.scitotenv.2020.143231.
Chagas, T.Q., Freitas, Í.N., Montalvão, M.F., Nobrega, R.H., Machado, M.R.F., Charlie-Silva, I., et al., 2021b. Multiple endpoints of polylactic acid biomicroplastic toxicity in adult zebrafish (Danio rerio). Chemosphere 277, 130279. https://doi.org/10.1016/J.CHEMOSPHERE.2021.130279.
Chen, J., Rao, C., Yuan, R., Sun, D., Guo, S., Li, L., Yang, S., et al., 2022a. Long-term exposure to polyethylene microplastics and glyphosate interferes with the behavior, intestinal microbial homeostasis, and metabolites of the common carp (Cyprinus carpio L.). Sci. Total Environ. 814, 152681 https://doi.org/10.1016/J.SCITOTENV.2021.152681.
Chen, X., Zhuang, J., Chen, Q., Xu, L., Yue, X., Qiao, D., 2022b. Chronic exposure to polyvinyl chloride microplastics induces liver injury and gut microbiota dysbiosis based on the integration of liver transcriptome profiles and full-length 16S rRNA sequencing data. Sci. Total Environ. 839, 155984 https://doi.org/10.1016/J.SCITOTENV.2022.155984.
Cialla-May, D., Krafft, C., Rösch, P., Deckert-Gaudig, T., Frosch, T., Jahn, I.J., Pahlow, S., et al., 2022. Raman spectroscopy and imaging in bioanalytics. Anal. Chem. 94, 86–119. https://doi.org/10.1021/ACS.ANALCHEM.1C03235.
Cueva, C., Jiménez-Girón, A., Muñoz-González, I., Esteban-Fernández, A., Gil-Sánchez, I., Dueñas, M., Martín-Álvarez, P.J., et al., 2015. Application of a new dynamic gastrointestinal simulator (SIMGI) to study the impact of red wine in colonic metabolism. Food Res. Int. 72, 149–159. https://doi.org/10.1016/j.foodres.2015.03.003.
Cueva, C., Gil-Sánchez, I., Tamargo, A., Miralles, B., Crespo, J., Bartolomé, B., Moreno-Arribas, M.V., 2019. Gastrointestinal digestion of food-use silver nanoparticles in the dynamic SIMulator of the GastroIntestinal tract (simgi®). Impact on human gut microbiota. Food Chem. Toxicol. 132, 110657 https://doi.org/10.1016/j.fct.2019.110657.
de Oliveira, J.P.J., Estrela, F.N., Rodrigues, A.S. de L., Guimarães, A.T.B., Rocha, T.L., Malafaia, G., 2021. Behavioral and biochemical consequences of Danio rerio larvae exposure to polylactic acid bioplastic. J. Hazard. Mater. 404 https://doi.org/10.1016/J.JHAZMAT.2020.124152.
Derrien, M., Turroni, F., Ventura, M., van Sinderen, D., 2022. Insights into endogenous Bifidobacterium species in the human gut microbiota during adulthood. Trends Microbiol. 30, 940–947. https://doi.org/10.1016/J.TIM.2022.04.004.
DeStefano, V., Khan, S., Tabada, A., 2020. Applications of PLA in modern medicine. Eng. Regen. 1, 76–87. https://doi.org/10.1016/J.ENGREG.2020.08.002.
Duan, Z., Cheng, H., Duan, X., Zhang, Haihong, Wang, Y., Gong, Z., Zhang, Huajing, et al., 2022. Diet preference of zebrafish (Danio rerio) for bio-based polylactic acid microplastics and induced intestinal damage and microbiota dysbiosis. J. Hazard. Mater. 429 https://doi.org/10.1016/J.JHAZMAT.2022.128332.
Elmowafy, E.M., Tiboni, M., Soliman, M.E., 2019. Biocompatibility, biodegradation and biomedical applications of poly(lactic acid)/poly(lactic-co-glycolic acid) micro and nanoparticles. J. Pharm. Investig. 49, 347–380. https://doi.org/10.1007/S40005-019-00439-X.
Farah, S., Anderson, D.G., Langer, R., 2016. Physical and mechanical properties of PLA, and their functions in widespread applications — a comprehensive review. Adv. Drug Deliv. Rev. 107, 367–392. https://doi.org/10.1016/j.addr.2016.06.012.
Fassarella, M., Blaak, E.E., Penders, J., Nauta, A., Smidt, H., Zoetendal, E.G., 2021. Gut microbiome stability and resilience: elucidating the response to perturbations in order to modulate gut health. Gut. https://doi.org/10.1136/gutjnl-2020-321747.
Fournier, E., Etienne-Mesmin, L., Grootaert, C., Jelsbak, L., Syberg, K., Blanquet-Diot, S., Mercier-Bonin, M., 2021. Microplastics in the human digestive environment: a focus on the potential and challenges facing in vitro gut model development. J. Hazard. Mater. 415, 125632 https://doi.org/10.1016/J.JHAZMAT.2021.125632.
Fournier, E., Leveque, M., Ruiz, P., Ratel, J., Durif, C., Chalancon, S., Amiard, F., et al., 2023a. Microplastics: what happens in the human digestive tract? First evidences in adults using in vitro gut models. J. Hazard. Mater. 442 https://doi.org/10.1016/j.jhazmat.2022.130010.
Fournier, E., Ratel, J., Denis, S., Leveque, M., Ruiz, P., Mazal, C., Amiard, F., et al., 2023b. Exposure to polyethylene microplastics alters immature gut microbiome in an infant in vitro gut model. J. Hazard. Mater. 443, 130383 https://doi.org/10.1016/j.jhazmat.2022.130383.
García-Villalba, R., Giménez-Bastida, J.A., García-Conesa, M.T., Tomás-Barberán, F.A., Carlos Espín, J., Larrosa, M., 2012. Alternative method for gas chromatography-mass spectrometry analysis of short-chain fatty acids in faecal samples. J. Sep. Sci. 35, 1906–1913. https://doi.org/10.1002/jssc.201101121.
Gewert, B., Plassmann, M.M., Macleod, M., 2015. Pathways for degradation of plastic polymers floating in the marine environment. Environ. Sci. Process. Impacts. https://doi.org/10.1039/c5em00207a.
Gil-Sánchez, I., Cueva, C., Sanz-Buenhombre, M., Guadarrama, A., Moreno-Arribas, M.V., Bartolomé, B., 2018. Dynamic gastrointestinal digestion of grape pomace extracts: bioaccessible phenolic metabolites and impact on human gut microbiota. J. Food Compos. Anal. 68, 41–52.
Godoy, V., Martínez-Férez, A., Martín-Lara, M.Á., Vellido-Pérez, J.A., Calero, M., Blázquez, G., 2020. Microplastics as vectors of chromium and lead during dynamic simulation of the human gastrointestinal tract. Sustainability 12, 4792. https://doi.org/10.3390/SU12114792.
Harata, G., Yoda, K., Wang, R., Miyazawa, K., Sato, M., He, F., Endo, A., 2021. Species- and age/generation-dependent adherence of bifidobacterium bifidum to human intestinal mucus in vitro. Microorganisms 9, 1–9. https://doi.org/10.3390/microorganisms9030542.
Hii, S.L., Tan, J.S., Ling, T.C., Ariff, A. Bin, 2012. Pullulanase: role in starch hydrolysis and potential industrial applications. Enzyme Res. 2012 https://doi.org/10.1155/2012/921362.
Horiue, H., Sasaki, M., Yoshikawa, Y., Toyofuku, M., Shigeto, S., 2020. Raman spectroscopic signatures of carotenoids and polyenes enable label-free visualization of microbial distributions within pink biofilms. Sci. Rep. 10 (1), 1–10. https://doi.org/10.1038/s41598-020-64737-3, 2020 10:
Huang, W., Yin, H., Yang, Y., Jin, L., Lu, G., Dang, Z., 2021b. Influence of the co-exposure of microplastics and tetrabromobisphenol A on human gut: simulation in vitro with human cell Caco-2 and gut microbiota. Sci. Total Environ. 778, 146264 https://doi.org/10.1016/J.SCITOTENV.2021.146264.
Huang, Z., Weng, Y., Shen, Q., Zhao, Y., Jin, Y., 2021a. Microplastic: a potential threat to human and animal health by interfering with the intestinal barrier function and changing the intestinal microenvironment. Sci. Total Environ. 785, 147365 https://doi.org/10.1016/J.SCITOTENV.2021.147365.
Huttenhower, C., Gevers, D., Knight, R., Abubucker, S., Badger, J.H., Chinwalla, A.T., Creasy, H.H., et al., 2012. Structure, function and diversity of the healthy human microbiome. Nature 486, 207–214. https://doi.org/10.1038/nature11234.
Jiménez-Arroyo, C., Tamargo, A., Molinero, N., Moreno-Arribas, M.V., 2023. The gut microbiota, a key to understanding the health implications of micro(nano)plastics and their biodegradation. Microb. Biotechnol. 16, 34–53. https://doi.org/10.1111/1751-7915.14182.
Jin, Y., Lu, L., Tu, W., Luo, T., Fu, Z., 2019. Impacts of polystyrene microplastic on the gut barrier, microbiota and metabolism of mice. Sci. Total Environ. 649, 308–317. https://doi.org/10.1016/j.scitotenv.2018.08.353.
Kister, G., Cassanas, G., Vert, M., 1998. Effects of morphology, conformation and configuration on the IR and Raman spectra of various poly(lactic acid)s. Polymer (Guildf) 39, 267–273. https://doi.org/10.1016/S0032-3861(97)00229-2.
Kister, G., Cassanas, G., Bergounhon, M., Hoarau, D., Vert, M., 2000. Structural characterization and hydrolytic degradation of solid copolymers of d,l-lactide-co-ε-caprolactone by Raman spectroscopy. Polymer (Guildf) 41, 925–932. https://doi.org/10.1016/S0032-3861(99)00223-2.
Klimenko, N.S., Odintsova, V.E., Revel-Muroz, A., Tyakht, A.V., 2022. The hallmarks of dietary intervention-resilient gut microbiome. NPJ Biofilms Microbiomes 8, 1–11. https://doi.org/10.1038/s41522-022-00342-8.
Krasucka, P., Bogusz, A., Baranowska-Wójcik, E., Czech, B., Szwajgier, D., Rek, M., Ok, Y. S., Oleszczuk, P., 2022. Digestion of plastics using in vitro human gastrointestinal tract and their potential to adsorb emerging organic pollutants. Sci. Total Environ. 843, 157108 https://doi.org/10.1016/J.SCITOTENV.2022.157108.
Kutralam-Muniasamy, G., Shruti, V.C., Pérez-Guevara, F., Roy, P.D., 2023. Microplastic diagnostics in humans: "the 3Ps" Progress, problems, and prospects. Sci. Total Environ. 856, 159164 https://doi.org/10.1016/j.scitotenv.2022.159164.
Li, X., Lin, Y., Liu, M., Meng, L., Li, C., 2022. A review of research and application of polylactic acid composites. J. Appl. Polym. Sci. https://doi.org/10.1002/app.53477.
Liu, Y., Gai, M., Sukvanitvichai, D., Frueh, J., Sukhorukov, G.B., 2020. pH dependent degradation properties of lactide based 3D microchamber arrays for sustained cargo release. Colloids Surf. B: Biointerfaces 188. https://doi.org/10.1016/J.COLSURFB.2020.110826.
Lloyd-Price, J., Abu-Ali, G., Huttenhower, C., 2016. The healthy human microbiome. Genome Medicine 8 (1), 1–11. https://doi.org/10.1186/S13073-016-0307-Y, 2016 8.
Lu, L., Wan, Z., Luo, T., Fu, Z., Jin, Y., 2018. Polystyrene microplastics induce gut microbiota dysbiosis and hepatic lipid metabolism disorder in mice. Sci. Total Environ. 631–632, 449–458. https://doi.org/10.1016/j.scitotenv.2018.03.051.
Maharana, T., Pattanaik, S., Routaray, A., Nath, N., Sutar, A.K., 2015. Synthesis and characterization of poly(lactic acid) based graft copolymers. React. Funct. Polym. 93, 47–67. https://doi.org/10.1016/J.REACTFUNCTPOLYM.2015.05.006.
Malafaia, G., Barceló, D., 2023. Microplastics in human samples: recent advances, hot-spots, and analytical challenges. TrAC Trends Anal. Chem. 161, 117016 https://doi.org/10.1016/j.trac.2023.117016.
Malafaia, G., Nascimento, Í.F., Estrela, F.N., Guimarães, A.T.B., Ribeiro, F., da Luz, T.M., Rodrigues, A.S. de L., 2021. Green toxicology approach involving polylactic acid biomicroplastics and neotropical tadpoles: (eco)toxicological safety or environmental hazard? Sci. Total Environ. 783, 146994 https://doi.org/10.1016/j.scitotenv.2021.146994.
Nguyen, N.H.A., Marlita, M., El-Temsah, Y.S., Hrabak, P., Riha, J., Sevcu, A., 2023. Early stage biofilm formation on bio-based microplastics in a freshwater reservoir. Sci. Total Environ. 858, 159569 https://doi.org/10.1016/J.SCITOTENV.2022.159569.
Nishiyama, K., Takaki, T., Sugiyama, M., Fukuda, I., Aiso, M., Mukai, T., Odamaki, T., et al., 2020. Extracellular vesicles produced by Bifidobacterium longum export mucin-binding proteins. Appl. Environ. Microbiol. 86 e01464-20.
Nishiyama, K., Yokoi, T., Sugiyama, M., Osawa, R., Mukai, T., Okada, N., 2021. Roles of the cell surface architecture of Bacteroides and Bifidobacterium in the gut colonization. Front. Microbiol. https://doi.org/10.3389/fmicb.2021.754819.

Oberbeckmann, S., Löder, M.G.J., Labrenz, M., 2015. Marine microplastic-associated biofilms - a review. Environ. Chem. 12, 551–562. https://doi.org/10.1071/EN15069.

Ouyang, M.Y., Feng, X.S., Li, X.X., Wen, B., Liu, J.H., Huang, J.N., Gao, J.Z., Chen, Z.Z., 2021. Microplastics intake and excretion: resilience of the intestinal microbiota but residual growth inhibition in common carp. Chemosphere 276, 130144. https://doi.org/10.1016/J.CHEMOSPHERE.2021.130144.

Pang, X., Zhuang, X., Tang, Z., Chen, X., 2010. Polylactic acid (PLA): research, development and industrialization. Biotechnol. J. https://doi.org/10.1002/biot.201000135.

Pezzotti, G., 2021. Raman spectroscopy in cell biology and microbiology. J. Raman Spectrosc. 52, 2348–2443. https://doi.org/10.1002/JRS.6204.

Qiao, J., Chen, R., Wang, M., Bai, R., Cui, X., Liu, Y., Wu, C., Chen, C., 2021. Perturbation of gut microbiota plays an important role in micro/nanoplastics-induced gut barrier dysfunction. Nanoscale 13, 8806–8816. https://doi.org/10.1039/D1NR00038A.

Qin, D., Kean, R.T., 1998. Crystallinity determination of polylactide by FT-Raman spectrometry. Appl. Spectrosc. 52, 488–495. https://doi.org/10.1366/0003702981943950.

Quast, C., Pruesse, E., Yilmaz, P., Gerken, J., Schweer, T., Yarza, P., Peplies, J., Glöckner, F.O., 2013. The SILVA ribosomal RNA gene database project: improved data processing and web-based tools. Nucleic Acids Res. 41, D590–D596. https://doi.org/10.1093/nar/gks1219.

Ramsperger, A.F.R.M., Bergamaschi, E., Panizzolo, M., Fenoglio, I., Barbero, F., Peters, R., Undas, A., Purker, S., et al., 2023. Nano- and microplastics: a comprehensive review on their exposure routes, translocation, and fate in humans. NanoImpact 29, 100441. https://doi.org/10.1016/J.IMPACT.2022.100441.

Rubio-Armendáriz, C., Alejandro-Vega, S., Paz-Montelongo, S., Gutiérrez-Fernández, Á. J., Carrascosa-Iruzubieta, C.J., Hardisson-de la Torre, A., 2022. Microplastics as emerging food contaminants: a challenge for food safety. Int. J. Environ. Res. Public Health 19, 1174. https://doi.org/10.3390/IJERPH19031174.

Ryan, S.M., Fitzgerald, G.F., Van Sinderen, D., 2006. Screening for and identification of starch-, amylopectin-, and pullulan-degrading activities in bifidobacterial strains. Appl. Environ. Microbiol. 72, 5289–5296. https://doi.org/10.1128/AEM.00257-06.

Sangeetha, V.H., Deka, H., Varghese, T.O., Nayak, S.K., 2018. State of the art and future prospectives of poly(lactic acid) based blends and composites. Polym. Compos. 39, 81–101. https://doi.org/10.1002/PC.23906.

Schmidt, T.S.B., Raes, J., Bork, P., 2018. The human gut microbiome: from association to modulation. Cell 172, 1198–1215. https://doi.org/10.1016/J.CELL.2018.02.044.

Schwabl, P., Koppel, S., Konigshofer, P., Bucsics, T., Trauner, M., Reiberger, T., Liebmann, B., 2019. Detection of various microplastics in human stool: a prospective case series. Ann. Intern. Med. 171, 453–457. https://doi.org/10.7326/M19-0618.

Senathirajah, K., Attwood, S., Bhagwat, G., Carbery, M., Wilson, S., Palanisami, T., 2021. Estimation of the mass of microplastics ingested – a pivotal first step towards human health risk assessment. J. Hazard. Mater. 404, 124004 https://doi.org/10.1016/j.jhazmat.2020.124004.

Smith, P.B., Leugers, A., Kang, S., Yang, X., Hsu, S.L., 2001. Raman characterization of orientation in poly(lactic acid) films. Macromol. Symp. 175, 81–94. https://doi.org/10.1002/1521-3900(200110)175:1<81::AID-MASY81>3.0.CO;2-1.

Stock, V., Fahrenson, C., Thuenemann, A., Dönmez, M.H., Voss, L., Böhmert, L., Braeuning, A., et al., 2020. Impact of artificial digestion on the sizes and shapes of microplastic particles. Food Chem. Toxicol. 135, 111010 https://doi.org/10.1016/j.fct.2019.111010.

Tamargo, A., Cueva, C., Álvarez, M.D., Herranz, B., Bartolomé, B., Moreno-Arribas, M.V., Laguna, L., 2018. Influence of viscosity on the growth of human gut microbiota. Food Hydrocoll. 77, 163–167. https://doi.org/10.1016/j.foodhyd.2017.09.031.

Tamargo, A., Molinero, N., Reinosa, J.J., Alcolea-Rodriguez, V., Portela, R., Bañares, M. A., Fernández, J.F., Moreno-Arribas, M.V., 2022. PET microplastics affect human gut microbiota communities during simulated gastrointestinal digestion, first evidence of plausible polymer biodegradation during human digestion. Sci. Rep. 12, 528. https://doi.org/10.1038/S41598-021-04489-W.

Tan, H., Yue, T., Xu, Y., Zhao, J., Xing, B., 2020. Microplastics reduce lipid digestion in simulated human gastrointestinal system. Environ. Sci. Technol. 54, 12285–12294. https://doi.org/10.1021/acs.est.0c02608.

Toussaint, B., Raffael, B., Angers-Loustau, A., Gilliland, D., Kestens, V., Petrillo, M., Rio-Echevarria, I.M., van den Eede, G., 2019. Review of micro- and nanoplastic contamination in the food chain. Food Addit. Contam., Part A. https://doi.org/10.1080/19440049.2019.1583381.

Vandeputte, D., De Commer, L., Tito, R.Y., Kathagen, G., Sabino, J., Vermeire, S., Faust, K., Raes, J., 2021. Temporal variability in quantitative human gut microbiome profiles and implications for clinical research. Nat. Commun. 12, 1–13. https://doi.org/10.1038/s41467-021-27098-7.

Vano-Herrera, K., Vogt, C., 2017. Degradation of poly(L-lactic acid) coating on permanent coronary metal stent investigated ex vivo by micro Raman spectroscopy. J. Raman Spectrosc. 48, 711–719. https://doi.org/10.1002/jrs.5111.

Wen, S., Zhao, Y., Wang, M., Yuan, H., Xu, H., 2022. Micro(nano)plastics in food system: potential health impacts on human intestinal system. Crit. Rev. Food Sci. Nutr. 1–19 https://doi.org/10.1080/10408398.2022.2116559.

Xu, P., Zhang, S.Y., Luo, Z.G., Zong, M.H., Li, X.X., Lou, W.Y., 2021. Biotechnology and bioengineering of pullulanase: state of the art and perspectives. World J. Microbiol. Biotechnol. 37, 1–10. https://doi.org/10.1007/S11274-021-03010-9.

Yan, Z., Liu, Y., Zhang, T., Zhang, F., Ren, H., Zhang, Y., 2022a. Analysis of microplastics in human feces reveals a correlation between fecal microplastics and inflammatory bowel disease status. Environ. Sci. Technol. 56, 414–421. https://doi.org/10.1021/ACS.EST.1C03924.

Yan, Z., Zhang, S., Zhao, Yonggang, Yu, W., Zhao, Yanping, Zhang, Y., 2022b. Phthalates released from microplastics inhibit microbial metabolic activity and induce different effects on intestinal luminal and mucosal microbiota. Environ. Pollut. 310, 119884 https://doi.org/10.1016/j.envpol.2022.119884.

Yang, S., Xie, X., Ma, J., He, X., Li, Y., Du, M., Li, L., et al., 2021. Selective isolation of bifidobacterium from human faeces using pangenomics, metagenomics, and enzymology. Front. Microbiol. 12 https://doi.org/10.3389/fmicb.2021.649698.

Yu, H., Shi, L., Fan, P., Xi, B., Tan, W., 2022. Effects of conventional versus biodegradable microplastic exposure on oxidative stress and gut microorganisms in earthworms: a comparison with two different soils. Chemosphere 307, 135940. https://doi.org/10.1016/J.CHEMOSPHERE.2022.135940.

Yuniarto, K., Purwanto, Y.A., Purwanto, S., Welt, B.A., Purwadaria, H.K., Sunarti, T.C., 2016. Infrared and Raman studies on polylactide acid and polyethylene glycol-400 blend. In: AIP Conference Proceedings. American Institute of Physics Inc. https://doi.org/10.1063/1.4945555

Zettler, E.R., Mincer, T.J., Amaral-Zettler, L.A., 2013. Life in the "plastisphere": microbial communities on plastic marine debris. Environ. Sci. Technol. 47, 7137–7146. https://doi.org/10.1021/ES401288X.

Zhang, B., Yang, X., Liu, L., Chen, L., Teng, J., Zhu, X., Zhao, J., Wang, Q., 2021a. Spatial and seasonal variations in biofilm formation on microplastics in coastal waters. Sci. Total Environ. 770, 145303 https://doi.org/10.1016/J.SCITOTENV.2021.145303.

Zhang, J., Wang, L., Trasande, L., Kannan, K., 2021b. Occurrence of polyethylene terephthalate and polycarbonate microplastics in infant and adult feces. Environ. Sci. Technol. Lett. 8, 989–994. https://doi.org/10.1021/ACS.ESTLETT.1C00559.

Zhang, N., Li, Y. bin, He, H.R., Zhang, J.F., Ma, G.S., 2021c. You are what you eat: microplastics in the feces of young men living in Beijing. Sci. Total Environ. 767, 144345 https://doi.org/10.1016/J.SCITOTENV.2020.144345.

Zhang, X., Wen, K., Ding, D., Liu, J., Lei, Z., Chen, X., Ye, G., et al., 2021d. Size-dependent adverse effects of microplastics on intestinal microbiota and metabolic homeostasis in the marine medaka (Oryzias melastigma). Environ. Int. 151, 106452 https://doi.org/10.1016/J.ENVINT.2021.106452.

Zhao, Y., Qin, Z., Huang, Z., Bao, Z., Luo, T., Jin, Y., 2021. Effects of polyethylene microplastics on the microbiome and metabolism in larval zebrafish. Environ. Pollut. 282, 117039 https://doi.org/10.1016/J.ENVPOL.2021.117039.